A Study on Two degree of freedom Nonlinear PID Temperature Control of a Chemical Batch Reactor Process

Mihret Chole Hebena

A Thesis Submitted to the Department of Electrical Power and Control Engineering

School of Electrical Engineering and Computing

Presented in Partial Fulfillment of Requirement for the Degree of Master's in Electrical Power and Control Engineering (Control Engineering)

Office of Graduate Studies

Adama Science and Technology University

September, 2024

Adama, Ethiopia

A Study on Two degree of freedom Nonlinear PID Temperature Control of Chemical Batch Reactor Process

Mihret Chole Hebena

Advisor: Prof. Gang Gyoo Jin

A Thesis Submitted to the Department of Electrical Power and Control Engineering

School of Electrical Engineering and Computing

Presented in Partial Fulfillment of Requirement for the Degree of Master's in Electrical Power and Control Engineering (Control Engineering)

Office of Graduate Studies

Adama Science and Technology University

September, 2024

Adama, Ethiopia

DECLARATION

I hereby declare that this Master Thesis entitled "**A Study on Two degree of freedom Nonlinear PID Temperature Control of Chemical Batch Reactor Process**" is my original work. That is, it has not been submitted for the award of any academic degree, diploma, or certificate in any other university. All sources of material that are used for this thesis have been duly acknowledged through citation.

Mihret Chole Hebena _____ _____

Name of student Signature Date

RECOMMENDATION OF ADVISOR

I, the advisor of this thesis, hereby certify that I have read the revised version of thesis entitled "**A Study on Two degree of freedom Nonlinear PID Temperature Control of Chemical Batch Reactor Process**" prepared under my guidance by Mihret Chole submitted in partial fulfillment of the requirements for degree of Masters of Science in electrical power and control engineering (control). Therefore, I recommend the submission of the revised version of thesis to the department following the applicable procedures.

Prof. Gang Gyoo Jin

_____	_____	_____
Advisor	Signature	Date

APPROVAL PAGE

I, the advisor of the thesis entitled "**A Study on Two degree of freedom Nonlinear PID Temperature Control of Chemical Batch Reactor Process**" and developed by Mihret Chole; here by certify that the recommendation and suggestions made by the board of examiners are appropriately incorporated into the final version of the thesis.

Prof. Gang Gyoo Jin

Advisor	Signature	Date

We, the undersigned, members of the Board of Reviewers of the thesis by Mihret Chole have read and evaluated the thesis proposal entitled "**A Study on Two degree of freedom Nonlinear PID Temperature Control of Chemical Batch Reactor Process**" and examined the candidate during open defense. This is, therefore, to certify that the thesis is accepted for partial fulfillment of the requirement of the degree of Master of Science in Control Engineering.

Chairperson	Signature	Date
Reviewer 1	Signature	Date
Dr. Riessom Weldegiorgis		21/09/2024
Reviewer 2	Signature	Date

Final approval and acceptance of the thesis is contingent upon the submission of its final copy to the Office of Postgraduate Studies (OPGS) through the Department Graduate Council (DGC) and School Graduate Committee (SGC).

Department Head	Signature	Date
School Dean	Signature	Date
Office of Postgraduate Studies, Dean	Signature	Date

ACKNOWLEDGEMENT

I extend my sincerest gratitude to the Almighty God for His boundless grace and blessings that have guided me throughout this journey. I am deeply indebted to my advisor, Professor Gang Gyoo Jin, for his unwavering support, invaluable guidance, and constant encouragement. His expertise, patience, and insightful feedback were instrumental in shaping this research. I would also like to express my sincere appreciation Mr. Minyamer Gelawe Wase for his valuable insights and knowledge sharing.

I am especially grateful to my elder brother, Mr. Kaleb Chole, for his generous financial support, which made it possible for me to undertake this Master's program. His belief in my abilities has been a constant source of motivation.

Finally, I would like to thank all my family and friends for their unconditional love, support, and sacrifices. Their encouragement has been a constant source of motivation.

Table of Contents

DECLARATION i
RECOMMENDATION OF ADVISOR ii
APPROVAL PAGE iii
ACKNOWLEDGEMENT iv
LIST OF TABLES viii
LIST OF FIGURE ix
LIST OF ACRONYMS x
ABSTRACT xi
CHAPTER ONE 1
INTRODUCTION 1
1.1 Background 1
1.2 Statement of the Problem 4
1.3 Objective of the Study 5
1.3.1 General Objective 5
1.3.2 Specific Objectives 5
1.4 Scope of the Study 5
1.5 Limitation of the Study 5
1.6 Motivation of the Study 6
1.7 Significant of the Study 7
1.8 Thesis Organizations 7
CHAPTER TWO 8
THEORETICAL BACKGROUND AND LITERATURE REVIEW 8
2.1 Chemical Reactor Overview 8
2.2 Chemical Batch Reactor 9
2.3 Temperature Control of Batch Reactor 11
2.3.1 Related Works on Temperature Control of Batch Reactor 12
CHAPTER THREE 16
MODELLING OF BATCH REACTOR PROCESS 16
3.1 Methodologies 16
3.2 Modeling of Chemical Batch Reactor Process 17
3.2.1 Total Mass Balance Equation 21
3.2.2 Component Balance Equation 22

3.2.3 Energy Balance Equation 24
3.3 Dimensionless of the Batch Process Parameters 25
3.4 Dynamic Analysis of a Batch Reactor Process 27
3.4.1 State Space Modeling for a Batch Reactor Process 27
3.4.2 Open-loop Analysis of a Batch Reactor Process 28
3.4.3 Equilibrium State 28
CHAPTER FOUR 31
DESIGN OF A TDOF NPID CONTROLLER FOR A BATCH REACTOR PROCESS 31
4.1 Existing Linear and Nonlinear Controllers 31
4.1.1 Linear PID Controller 31
4.1.2 Nonlinear PID Controller 34
4.2 Design of a TDOF NPID Controller 36
4.2.1 NPID controller with a PD-type feedforward compensator 36
4.4 Optimal Tuning of the TDOF NPID Controller 38
4.4.1 PSO algorithm as an optimization tool 39
4.4.2 Performance Index 42
CHAPTER FIVE 44
SIMULATION RESULT AND DISCUSSION 44
5.1 Parameters of the Batch Reactor 44
5.2 Controller Parameter Settings 46
5.3 Results of the TDOF NPID Controller 47
5.3.1 Setpoint Tracking Response 47
5.3.2 Disturbance Rejection Response 48
5.4 Results of the NPID Controller 50
5.4.1 Setpoint Tracking Response 50
5.4.2 Disturbance Rejection Response 51
5.5 Results of the PID Controller 52
5.5.1 Setpoint Tracking Response 52
5.5.2 Disturbance Rejection Response 53
5.6 Performance Comparison of the Three Controllers 54
5.6.1 Setpoint Tracking Performance 54
5.6.2 Disturbance Rejection Performance 55
CHAPTER SIX 57

CONCLUSION AND RECOMMENDATION 57
6.1 CONCLUSION.....57
REFERENCES 59

LIST OF TABLES

Table 5.1 Process parameters and values (Chen, 2014).....45
Table 5.2 Parameters of the PSO algorithm 46
Table 5.3 Optimum settings of PID-TL, NPID and TDOF NPID controllers 47
Table 5.4 Setpoint tracking performance of the three controllers.....55
Table 5.5 Disturbance rejection performance of the three controllers 56

LIST OF FIGURE

Figure 1.1 Chemical batch reactor tank (University of Michigan, 2022).....3
Figure 2.1 Schematic diagram of a batch reactor (Ahmed, 2013).....10
Figure 3.1 Schematic representation of the research process.....16
Figure 3.2 Batch process (Chen & Peng, 1998).....18
Figure 3.3 Concentration-time plot.....19
Figure 4.1 Structure of the proposed Batch Reactor temperature control system.....31
Figure 4.2 Schematic diagram of the PID controller (Halim & Ismail, 2019).....32
Figure 4.3 The PID control system.....34
Figure 4.4 Graphical representation of v(t) for typical values of σ = 1.5, 1.0 and 0.5. 35
Figure 4.5 The NPID control system.....36
Figure 4.6 TDOF NPID control system with a feedforward compensator u_f.....37
Figure 4.7 Equivalent TDOF NPID control system. 38
Figure 4.8 Flow chart of PSO algorithm 40
Figure 4.9 TDOF NPID controller tuning using PSO 42
Figure 5.1Step response of the TDOF NPID controller 47
Figure 5.2 Disturbance rejection response of the TDOF NPID 49
Figure 5.3 Step responses of the NPID controller.....50
Figure 5.4 Disturbance rejection of the NPID controller 51
Figure 5.5Step responses of the PID controller.....52
Figure 5.6 Disturbance Rejection of PID-TL controller.....53
Figure 5.7 The three controllers' step responses.....54
Figure 5.8 Disturbance rejection responses of the three controllers.....55

LIST OF ACRONYMS

TL	Tyreus-Luyben
PSO	Particle Swarm Optimization
IAE	Integral Absolute Error
ITAE	Integral of Time Absolute Error
ISE	Integral Squared Error
ITSE	Integral of Time Square Error
TDOF	Two-degree-of-freedom
NPID	Nonlinear Proportional Integral and Derivative
PID	Proportional Integral and Derivative

ABSTRACT

The Batch reactor is a popular equipment used in a variety of process industries to create a wide range of products. It is a sealed receptacle used for a non-continuous chemical reaction. Unlike a continuous reactor where materials constantly flow in and out, a batch reactor holds all the ingredients (reactants) from the start. This made extremely difficult by the complex and unpredictable behavior of chemical reactions and their tendency to become unstable. This thesis investigates the application of a Two degree of freedom Nonlinear PID controller for a Chemical Batch Reactor process. The batch reactor process is mathematically represented by the mass and energy balance within the reactor. The parameters of TDOF NPID's settings were fine-tuned using a Particle Swarm Optimization technique. Its effectiveness was measured by calculating the Integral Absolute Error. The outcomes of simulations show how well the suggested controller maintains the desired temperature (setpoint tracking) and minimizes the impact of external temperature fluctuations (disturbance rejection). A comparative analysis with two existing works (PID and nonlinear PID controller) is investigated. Simulation results indicate that the proposed Two degree of freedom Nonlinear PID controller surpasses existing control systems. For setpoint tracking, it achieved a settling time of 25.51 with 28.46% overshoot and an IAE of 159.37. In terms of disturbance rejection, the controller exhibited a recovery time of 2.89, a peak overshoot of 0.05%, and an IAE of 0.05. The results were compared to those of a Nonlinear PID and a Conventional PID controller.

Keywords: *Chemical batch reactor, Temperature control, NPID controller, TDOF NPID controller, PSO.*

CHAPTER ONE

INTRODUCTION

1.1 Background

One sector of the economy is the chemical industry, which uses a range of natural resources as basic raw materials to make highly valuable compounds. The construction and management of chemical reactors are essential to the chemical industry, serving as the foundational technology for enabling chemical reactions. Chemical science and technology are centered on the chemical transformation of materials, or chemical reaction (Tominaga & Tamaki, 1997).

Chemical reactors are the cornerstone of the chemical industry, serving as vessels where controlled chemical transformations occur. These engineered environments facilitate the conversion of raw materials into valuable products through precise manipulation of reaction conditions such as temperature, pressure, and reactant concentrations. From the production of pharmaceuticals and fuels to the synthesis of advanced materials, chemical reactors underpin numerous technological advancements. Their design and operation are critical in optimizing product yield, minimizing waste, and ensuring process safety (Levenspiel, 2013)

Chemical reactions within a reactor can be either exothermic or endothermic, depending on their energy transfer. In exothermic reactions, the process releases heat to the surroundings, causing the reactors temperature to rise. Conversely endothermic reactions absorb heat from the surroundings, making the reactor cooler (Moran & Henkel, 2000).

Chemical reactors come in various forms depending on how they operate and manage the reacting chemicals. Broadly, they can be classified based on whether they run in batches (ingredients added all at once) or continuously (reactants constantly fed in products withdrawn). The reactor can also be designed for reaction where all the ingredients are in the same state (homogeneous) or separate states (heterogeneous, often requiring a catalyst) (Hill & Root, 2014). Within these categories, factors like how the chemicals flow through the reactor (well-mixed or plug flow) and how heat is managed further influence the specific reactor design. Ultimately, the right reactor type depends on the unique characteristics of the desired chemical reaction and the production goals.

Certain statistics indicate that batch-type procedures account for half of all manufacturing processes in the industry. (Štampar et al., 2013). Chemical batch reactor is a closed vessel that chemical reaction occurs. It operates as closed systems with no material entering or leaving the vessel during the reaction (Haan, 2015). All the reactants are introduced into the vessel at the beginning, and the reaction proceeds with nothing coming into or going out of the container until the process is complete. Inside the reactor the composition of the reaction mixture constantly changes making it an unsteady state process.

(Moran & Henkel, 2000)While continuous reactors reign supreme for large-scale production due to cost-effectiveness, batch reactors shouldn't be discounted, especially for smaller batches. Their simpler design with less equipment and lower control system coats make them ideal, even if they require more manpower. This versatility is particularly valuable in the dyestuff, fine chemical and pharmaceutical industries, allowing for the production of various products in the same reactor.

A batch reactor consists of several key components, each playing a crucial role in the reaction process. The main parts are reactor vessel, agitator, heating/cooling system, headspace, inlet/outlet valves, monitoring and control system (optional). The agitator stirs them into a well-mixed concoction (a mixture of various ingredients), and a heating/cooling jacket keeps the temperature just right. The headspace above the mixture provides room for volume changes, while inlet/outlet valves control the flow of materials. Some reactors even have monitoring and control systems to ensure everything runs smoothly, making batch reactors versatile tools for diverse chemical processes. Batch reactor process used in diary industry can be seen in Figure 1.1.

Figure 1.1 Chemical batch reactor tank (University of Michigan, 2022)

Batch reactor processes are inherently non-linear due to dynamic changes in reactant concentrations and reaction rates. Heat transfer, influenced by exothermic or endothermic reactions, further complicates temperature control. The interplay between these factors often leads to temperature fluctuations, compromising product quality and reaction efficiency. Precise temperature control is essential to overcome these challenges and optimize batch reactor performance (Global, 2023).

Furthermore, non-linear heat transfer within the reactor itself can create hot and cold spots due to factors like changing viscosity (fluid's resistance to flow) or uneven mixing. Unlike continuous reactors with more easily maintained conditions, batch processes experience a constantly evolving environment. This dynamic nature necessitates adjustments to temperature control strategy throughout the batch cycle, making a fixed approach impractical. In essence, the interplay between ever-changing reactant concentrations, limitation of heating/ cooling systems, nonlinear heat transfer, and the inherent dynamism of batch processes creates a complex web of challenges for maintaining critical temperature control. This control is crucial because temperature significantly impacts reaction rates, product yield, and ultimately the quality of the final product (Mann, 2009).

PID controllers, due to their simplicity and effectiveness, have become the industry standard for temperature control. These controllers regulate temperature by calculating an error between the setpoint and process variable, then adjusting control output accordingly (Štampar et al., 2013). While PID controllers excel in many applications, their performance

can be limited in complex processes like batch reactors due to non-linear dynamics (Yadav et al., 2021). To address the challenges associated with batch reactor temperature control, advanced control strategies that offer greater flexibility and adaptability are essential. Optimization techniques like Genetic Algorithms and Particle Swarm Optimization can further enhance controller performance.

This research investigates the application of a Two-Degree-of-Freedom (TDOF) Nonlinear Proportional-Integral-Derivative (NPID) controller for temperature control within a chemical batch reactor. The TDOF architecture, combined with nonlinear control strategies, offers the potential for improved performance in handling the inherent nonlinearities and disturbances prevalent in chemical processes. The proposed TDOF NPID controller is rigorously evaluated against traditional PID and NPID controllers without the TDOF architecture. The evaluation examines how well the controller handles both steady-state errors and transient responses, including its ability to follow target values and counteract external influences. This research aims to demonstrate the proposed controller's competitive performance in both disturbance rejection and set-point tracking. Its ability to minimize overshoot and integral absolute error (IAE) during disturbance rejection, coupled with its effective tracking of set-point changes, can be particularly beneficial in applications where precise temperature control is critical.

1.2 Statement of the Problem

Achieving precise temperature control in chemical batch reactors is a critical yet challenging task due to the inherent non-linear dynamics and external disturbances. Traditional linear control strategies, such as PID controllers, often struggle to maintain desired temperature profiles in the face of changing reaction conditions and external fluctuations. While advanced control techniques offer potential solutions, their implementation often requires complex modeling and tuning processes. This research proposes a TDOF-NPID controller, a simpler and adaptive approach that aims to overcome the challenges associated with advanced controller modeling. The controller seeks to achieve temperature control while minimizing the complexity and computational burden typically associated with more sophisticated techniques. PSO is used for tuning the settings of the controller in order to attain maximum performance. The entire system, including the reactor model and the stated

controller, is then simulated within the MATLAB software environment to assess its potential effectiveness.

1.3 Objective of the Study

1.3.1 General Objective

The main goal of this research is to develop a TDOF NPID controller for regulating temperature in a chemical batch reactor process, utilizing particle swarm optimization for parameter tuning.

1.3.2 Specific Objectives

Particular goals are to:

- Construct a nonlinear model describing the behavior of the chemical batch reactor.
- Design a TDOF NPID controller architecture for the temperature control of the chemical batch reactor.
- Tune the controller parameters using PSO.
- Evaluate the controller's effectiveness in a simulated environment and compare its performance with NPID and PID controllers.

1.4 Scope of the Study

The inquiry focuses on the design, optimization, and evaluation of a TDOF NPID controller for precise temperature control within a specific chemical batch reactor. A nonlinear model of the reactor capturing key temperature dynamics will be developed. The TDOF NPID controller architecture, incorporating non-linear elements and separate control loops, will be designed. Performance evaluation in a simulated reactor environment will assess setpoint tracking, disturbance rejection, and transient state behavior. The proposed controller's effectiveness will be compared to traditional PID and potentially a non-linear PID controller without TDOF architecture.

1.5 Limitation of the Study

Due to the focus on a simulated reactor environment, this study inherently possesses limitations when compared to a real-world chemical batch reactor. While a nonlinear model will be developed to capture the core temperature dynamics of the reactor, it might not fully account for all the complexities that arise in a physical system. Accurately determining the

model parameters, such as reaction rate constants and heat transfer coefficients, can be challenging. These parameters can vary based on the specific reactor setup, feedstock composition, and operating conditions. Reliance on estimations from literature or limited experimental data introduces some uncertainty into the model's accuracy in predicting reactor activity.

Furthermore, the study might not capture the full range of potential disturbances or process variability that a real batch reactor might encounter. Chemical batch reactors can exhibit some level of variability due to factors like slight differences in equipment or fluctuations in feedstock composition. The model might assume constant or average values for these parameters, potentially leading to discrepancies when applied to a specific reactor setup. Additionally, certain parameters within the reactor, like reaction rate constants or heat transfer coefficients, might change subtly throughout the batch cycle. The model might not account for these dynamic changes, potentially affecting the controller's performance in real-time operation. Unforeseen events like equipment malfunctions or changes in ambient conditions could introduce additional challenges for the controller in a real system that the study might not encompass.

These limitations highlight the importance of future work on model refinement to capture the complexities of real-world batch reactor behavior. Refining methods for parameter estimation and real-world validation against actual reactor data will be crucial for ensuring the effectiveness of the controller in practical applications.

1.6 Motivation of the Study

Precise temperature control in chemical batch reactors is essential however conventional control methods often struggle to achieve this due to the inherent nonlinearities and disturbances present in the process. Advanced control techniques, while potentially offering improved performance, can be complex to model and tune. This study investigates a TDOF NPID controller as a promising alternative. By leveraging its simplicity and adaptability, the TDOF NPID controller aims to overcome the challenges associated with traditional and advanced control methods, providing a solution for temperature control in chemical batch reactors.

1.7 Significant of the Study

Conventional controllers often struggle with nonlinear systems, while advanced control techniques frequently require complex modeling processes. This research aims to address the critical challenge of temperature control in chemical batch reactors. By leveraging its reduced complexity and adaptability, this research investigates the effectiveness of the TDOF NPID controller in controlling the temperature of chemical batch reactors. This means to evaluate how well the TDOF NPID controller can regulate temperature in chemical batch reactors and providing valuable insights for future research and applications.

1.8 Thesis Organizations

The thesis consists of six chapters.

Chapter 2: Offers a literature survey exploring the context of chemical batch reactor processes and different temperature control techniques.
Chapter 3: Develops mathematical models for Chemical batch reactor.
Chapter 4: Presents the design of the proposed TDOF NPID controller for temperature control.
Chapter 5: Analyzes simulation results, evaluates controller performance, and compares it to existing methods. Discusses the limitations of the findings.
Chapter 6: Summarizes key findings, reiterates significance and contributions. Provides recommendations for future research and potential applications.

CHAPTER TWO

THEORETICAL BACKGROUND AND LITERATURE REVIEW

2.1 Chemical Reactor Overview

Chemical reaction engineering (CRE) deals with the design, operation, and selection of reactors for various chemical transformations. In the realm of chemical engineering, a vital piece of equipment is the chemical reactor. It serves as the reaction chamber where various chemical transformations take place (Skogestad, 2008).

These transformations convert raw materials (reactants) into desired products. The vast diversity of reactor types, operating conditions, and influencing factors necessitates a broad understanding of control strategies to optimize reactor performance. These carefully designed vessels act as the stage for chemical reactions, emulating the vital role of a heart by continuously pumping out the building blocks for countless materials from fuels and plastics to pharmaceuticals and fertilizers. Without reactors, these transformations would be impossible, as uncontrolled reactions often yield unwanted byproducts or inefficient conversions (Mann, 2009).

(Scott Fogler, 2016)Moreover, advancements in reactor design and control strategies continue to push the boundaries of what's achievable, fostering innovation and technological progress across various sectors. In essence, chemical reactors are the engines of industrial transformation, driving the efficient and sustainable production of the materials that define our world.

Chemical reactors are classified according to their operational mode, with three main types: batch, continuous, and plug flow. Batch reactors work in a cyclical method, consuming a specific amount of reactants at a time. A certain quantity of reactants is injected into the reactor vessel (Missen et al., 1999). Once loaded, the reactor is closed and the reaction proceeds to run out under controlled conditions for a predetermined time. This method allows for more flexibility in adjusting reaction conditions between batches, but it requires downtime to clean and reload the reactor (Hill & Root, 2014).

Conversely, continuous reactors excel in high-volume production by constantly processing a flowing stream of reactants. However, this continuous operation provides less flexibility

for adjusting reaction parameters during processing. Finally, plug flow reactors operate by pushing reactants through a long, defined channel. This design mimics the movement of a "plug" of material, ensuring a specific order of events for the reaction and maximizing efficiency for reactions that benefit from such a sequence. Selecting the appropriate operational mode for a given chemical process is crucial for optimizing reaction performance and achieving desired product characteristics (Ravi, 2017).

2.2 Chemical Batch Reactor

Chemical Batch Reactor is a closed vessel that processes definite quantities, or batches, of reactants. In contrast to continuous reactors, which have a steady flow, batch reactors function in a discontinuous way and go through transitory processes. This enables modifications to reaction parameters (temperature, pressure, and catalyst) between batches (Kanavalau et al., 2019).This reactor also has intrinsic safety advantages, which are especially useful when dealing with dangerous or extremely exothermic processes. The reaction mixture is separated within the sealed vessel, reducing possible dangers when compared to continuous reactors in which reactants are always flowing. This advantage is especially important for generating new reactions involving new substances or unknown chemistry. Batch reactors continue to be used in a variety of applications. They are the preferred choice for high-value pharmaceuticals and specialty chemicals since they have complete control over reaction circumstances and product (Balaton et al., 2013).

At the heart of the action lies the motor (Doble, 2007), providing the power to drive the impeller, a rotating blade responsible for stirring the reaction mixture. The impeller's design and speed, which can be regulated by a speed reducer if necessary, ensure thorough mixing and optimal reactant contact.

Strategically placed within the reactor vessel are baffles. These internal walls disrupt swirling motions, preventing uneven mixing and vortex formation that could hinder the reaction (Smith, 2005). Maintaining the desired reaction temperature is crucial, and this is achieved through the jacket. This double wall allows for the circulation of heating or cooling fluids through connections, ensuring a stable thermal environment for the reaction (Smith, 2005). Finally, the shaft transmits the motor's power to the impeller, and the drain valve allows for the controlled discharge of the reaction mixture once the process is complete.

Each component plays a vital role in the intricate dance within the batch reactor, ultimately leading to the successful production of specialty chemicals (Doble, 2007; Smith, 2005).

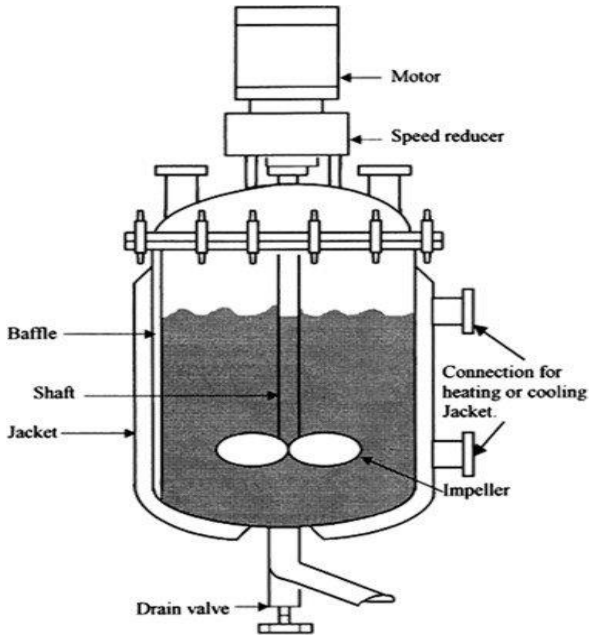

Figure 2.1 Schematic diagram of a batch reactor (Ahmed, 2013)

The batch reactor, a powerhouse in making special chemicals, carries out a carefully planned series of changes. At its core lies the reaction vessel, a robust and often pressurized container. Constructed from materials like steel or glass-lined steel to withstand the demanding reaction conditions (temperature, pressure) (Schmidt, 2005), this vessel serves as the reaction chamber, housing the transformative dance of chemicals. The size of the reactor vessel can vary considerably, ranging from a few liters employed in research settings to tens of thousands of liters utilized in large-scale industrial applications (Shuler, 1992).

Within this reaction chamber resides the reaction medium. This medium comprises a carefully formulated mixture of the starting materials, or reactants that will undergo the desired chemical transformation. To ensure the efficiency and success of the reaction, thorough mixing of these reactants is paramount. This critical task falls to the agitator, a component specifically designed to continuously stir the reaction medium (Shuler, 1992). The agitator's design, often featuring impellers (paddle-like blades) or turbines (propeller-like blades), promotes uniform distribution of the reactants throughout the reaction chamber and prevents the formation of stagnant zones where the reaction might not proceed as effectively (Schmidt, 2005).

An additional element within the reactor vessel is the headspace. This seemingly empty space situated above the reaction medium serves a vital purpose. As the reaction progresses, some of the reactants might be converted into gaseous products. The headspace accommodates this volume expansion, preventing excessive pressure buildup within the vessel and ensuring safe operation (Shuler, 1992). Furthermore, the agitator plays a dual role by facilitating the transfer of heat generated or absorbed during the reaction. This heat exchange can occur through the vessel walls or through the reaction medium itself, ensuring the reaction proceeds at the optimum temperature for efficient product formation (Schmidt, 2005).

Keeping the perfect temperature is the key for a successful outcome. A double wall around the pot acts like a heating and cooling system. By circulating hot or cold liquids through tubes, this jacket keeps the temperature just right for the reaction. All along, a team of sensors acts like observers, constantly checking on how things are going. They track things like temperature, pressure, and how far the reaction has come. This information helps the controller, like a stage manager, make adjustments if needed, maybe by changing the mixing speed or the temperature control system (Toledo & Mettler, 2024).

Once the reaction is all done, as decided beforehand, it's time to empty the pot. A drain valve opens, letting the mixture flow out. The product, which might need some extra cleaning, takes its final step. Finally, the pot gets a good scrub down, getting ready for the next batch. With each carefully planned change inside the batch reactor, raw materials are transformed into valuable specialty chemicals.

2.3 Temperature Control of Batch Reactor

A batch process is inherently a dynamic system, characterized by transient changes in process variables over time. Unlike continuous processes operating under steady-state conditions (Z. Zhang et al., 2018), batch processes involve dynamic trajectories requiring precise control. The necessity of accurately tracking desired process paths while simultaneously mitigating the impact of external disturbances. Robust control strategies are essential to achieve these objectives and ensure consistent product quality across batches.

Absence of Steady State in batch reactor process is because of dynamic Nature and discrete operation of the batch process. This undergo transient conditions, with process variables constantly changing over time. This dynamic behavior precludes the establishment of a steady state, where system variables remain constant. Batch processes involve distinct phases (charging, heating, reacting, cooling, discharging), each with its own set of conditions, preventing the attainment of a stable equilibrium. Because the system lacks a fixed equilibrium point, the reaction mixture's composition is continually changing as the reactants are depleted, while the products are generated. This dynamic state inhibits the system's progression toward chemical equilibrium.

In essence, the transient nature and finite duration of batch processes distinguish them from continuous processes, which operate under steady-state conditions and can potentially reach equilibrium.

2.3.1 Related Works on Temperature Control of Batch Reactor

Researchers have continuously explored various control strategies to achieve this vital objective. This section reviews recent advancements in temperature control for batch reactors, highlighting both established methods and emerging techniques, while also identifying potential limitations.

This research by (Ghasem et al., 2006) tackles temperature control in a batch reactor for polymerizing styrene. They use Model Predictive Control (MPC), a powerful technique that predicts future behavior to optimize control actions. This allows for a precise temperature profile, crucial for high-quality polymer. However, the study focuses on polystyrene production, and its effectiveness for other polymers might need further exploration.

This study by (Chen, 2014) proposes a model-based sliding mode control (SMC) strategy for precise temperature control in batch reactors. The controller design incorporates the reactor's mathematical model, allowing it to handle uncertainties and achieve robust performance. However, the development of accurate models for complex batch reactor processes can be challenging, and tuning the SMC parameters can be time-consuming. Additionally, designing SMC controllers can be complex due to the need to select appropriate sliding surfaces and determine the switching gains. Despite these limitations, the authors demonstrate the effectiveness of their approach through simulations, comparing

it to other control methods. Their results suggest that SMC offers a promising solution for maintaining desired temperature profiles in batch reactors despite variations in operating conditions and disturbances, provided that the model, parameters, and controller design are carefully considered.

(Štampar et al., 2013) proposes a novel control algorithm for batch reactor temperature control. This method combines a nonlinear PI controller with feed-forward action cascaded with a proportional (P) controller. The goal is to increase the efficiency of manufacturing by lowering control costs while improving product quality and quantity. The algorithm is designed to handle the complexities of batch reactors, including constraints and mixed discrete/continuous processes, by manipulating heating and cooling variables. The paper demonstrates the algorithm's stability and robustness through mathematical analysis and compares its performance to the standard cascade PI control used in industry, showing significant improvement in simulations.

Additionally, the study reports successful real-time implementation on a bioreactor. But a gap exists regarding generalizability. The algorithm's effectiveness in other reactor types (chemical, pharmaceutical, food) and its potential for optimization based on industry-specific priorities (yield, reaction time) remain unclear. Addressing these questions would broaden the understanding of this new control method's applicability across various batch reactor applications.

(Xiao et al., 2015) propose a Dynamic Matrix Control (DMC) strategy for batch reactor temperature control. This method adapts PID controller settings based on real-time conditions, addressing challenges like time delays and parameter variations. Simulations show improved performance compared to traditional PID control. However, the computational intensity of DMC modeling, which requires the inversion of a large matrix, can be a limitation. Additionally, the accuracy of the DMC model is crucial for achieving optimal performance, and developing such models can be challenging for complex batch reactor systems.

(Kadu et al., 2018) introduce a Sliding Mode Control (SMC) technique that uses a unique sliding surface to regulate unpredictable process control systems. This architecture relies on a linear state model and a performance index for optimal control, considers matched

uncertainties for stability, and is validated through simulations and real-world experiments. While this approach offers advantages, the reliance on a linear state model could limit applicability in highly non-linear systems. Additionally, the use of a state observer, which is necessary to estimate the system's internal states, can add complexity to the controller design and implementation.

(Narwekar & Shah, 2020) conduct a practical exploration of temperature control for batch reactors, investigating the application of Sliding Mode Control (SMC). They implement a traditional SMC control law and compare its effectiveness with a modified reaching law variant. While the study demonstrates SMC's potential for real-world control, it highlights a gap in understanding the specific impact of the modified reaching law on performance. Additionally, SMC design can be complex, involving the selection of appropriate sliding surfaces and determining switching gains. Furthermore, SMC can exhibit chattering behavior, characterized by high-frequency switching and sensitivity to noise, which can degrade performance and potentially damage actuators. The computational complexity associated with SMC implementation can also be a challenge.

(Gharagozloo et al., 2020) investigate the use of both sliding mode control (SMC) and nonlinear model predictive control (NMPC) to manage temperature in a chemical batch reactor. While NMPC minimizes the difference between predicted temperature and a desired profile, and SMC offers robustness against disturbances, the paper does not explicitly address how these two control methods can be effectively combined. While both techniques have their strengths, the research gap lies in how they could be strategically integrated to achieve superior temperature control. One potential approach could involve using NMPC for overall temperature control, with SMC as a backup to tackle unexpected changes. This integration could potentially lead to improved disturbance rejection, enhanced tracking accuracy, and even reduced computational load on NMPC. However, it's important to note that both SMC and NMPC can be computationally complex, especially for large-scale batch reactor systems.

This study by (Shamsuzzoha & Raja, 2023) examine the usage of neural networks-based PID (NNPID) and the Hammerstein Model-based Nonlinear PID (HNPID) as two control strategies for temperature management in a batch reactor used for acrylamide polymerization. HNPID utilizes a polynomial model to capture nonlinearities, while NNPID

employs a neural network to optimize PID gains. Both controllers were evaluated in simulations, with HNPID demonstrating superior tracking performance and lower energy consumption compared to NNPID. While simulations show HNPID performs better, a gap exists in selecting the optimal controller for specific situations. Factors like reaction complexity, computational resources, and required expertise could influence the choice. Additionally, both NNPID and HNPID have their limitations. NNPID can be computationally intensive, especially for complex neural networks, while the modeling of the Hammerstein model and tuning its parameters can also be challenging. Addressing these limitations, along with the need to assess the applicability of these controllers to other batch reactor systems beyond acrylamide polymerization, would provide a more comprehensive framework for selecting and tuning the most suitable controller for various batch reactor applications.

While TDOF NPID control offers potential advantages, its application to batch reactor temperature regulation seems less explored. As a relatively new technique, it might not have been widely studied or applied in this specific context yet. This research explores the use of a TDOF PID controller to address nonlinearities in plant dynamics. Building upon traditional PID controllers, it offers enhanced performance by incorporating nonlinear elements and providing flexibility through independent tuning of setpoint tracking and disturbance rejection. Unlike nonlinear PID, which focuses solely on handling nonlinearities, TDOF nonlinear PID leverages this advantage while offering additional degrees of freedom for improved control. Compared to more complex advanced control techniques, TDOF NPID offers a simpler approach for temperature regulation in batch reactors. This combination makes it a promising choice for processes with complex dynamics where traditional PID controllers might fall short.

CHAPTER THREE

MODELLING OF BATCH REACTOR PROCESS

The current section covers mathematical modeling of a chemical batch reactor using empirical information.

3.1 Methodologies

To accomplish the previously stated general and specific study objectives, the following methodological approaches will be utilized.

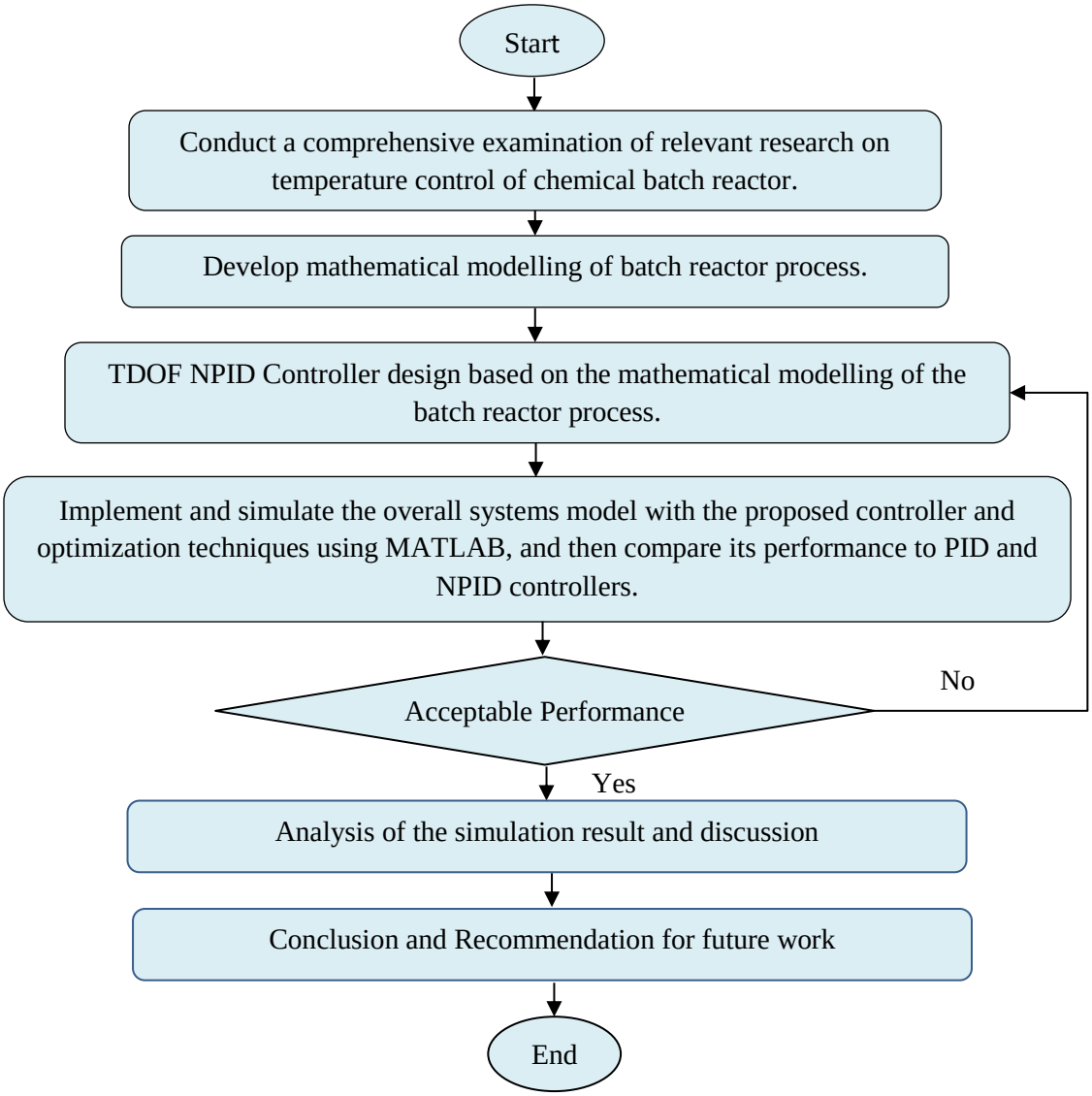

Figure 3.1 Schematic representation of the research process

A comprehensive review of relevant literature and research papers are conducted. Pertinent information is extracted and analyzed for this study. Following this, a mathematical model of the batch reactor process is created, and its stability is analyzed using equilibrium state equations. To regulate the reactor's temperature, a TDOF NPID controller is designed. The system's performance is evaluated through MATLAB simulations, comparing the outcomes with two existing PID and NPID controllers' strategies. Finally, the research concludes with a comprehensive analysis and recommendations for future work.

3.2 Modeling of Chemical Batch Reactor Process

A batch reactor undergoes two sequential, $A \xrightarrow{k_1} B \xrightarrow{k_2} C$ irreversible reactions. The first reaction $A \rightarrow B$ follows a second-order kinetic model, additionally the second reaction $B \rightarrow C$ follows a first-order kinetic model, where k_1 and k_2 are the rate constants for the conversion of A to B and B to C, respectively (Chen, 2014). This nonlinear relationship introduces nonlinearity into the overall system dynamics.

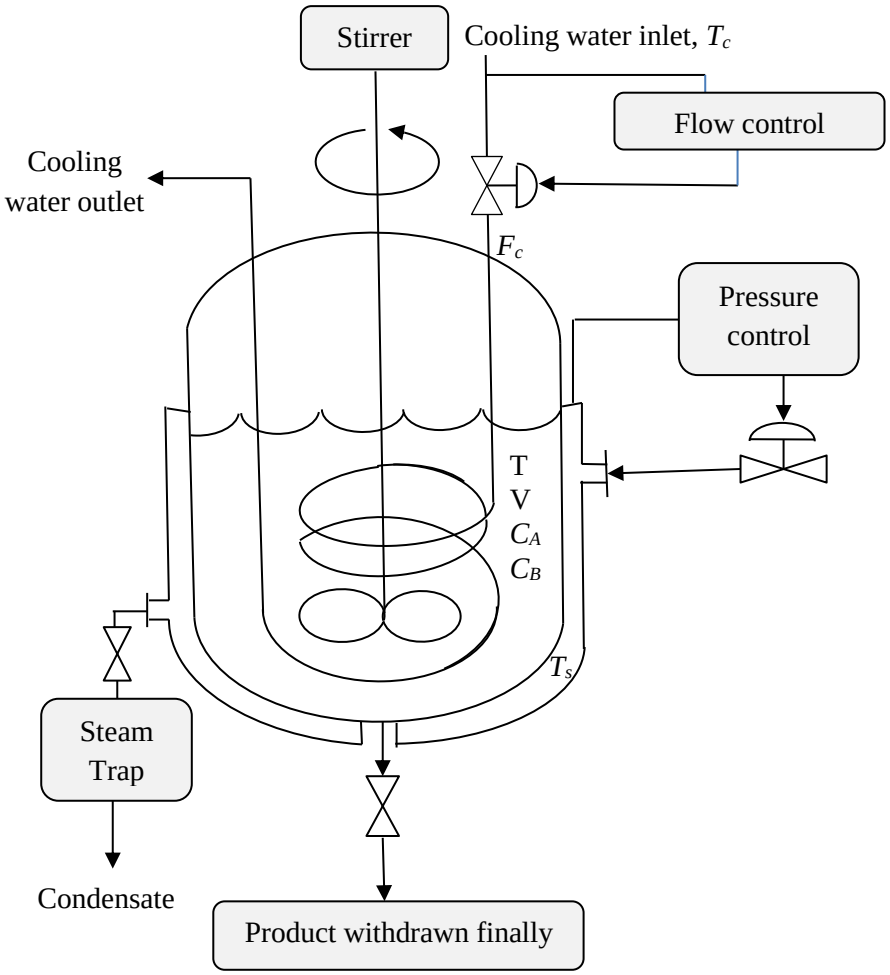

Figure 3.2 Batch process (Chen & Peng, 1998)

This study (Chen, 2014) investigates the optimization of intermediate product B formation within a sequential reaction pathway conducted within jacketed batch reactor. Because the batch system is isolated, there is no continuous outflow of material. Under conditions of ideal mixing within the reactor, the temperature and concentration profiles can be modeled as if there were an exit stream. A key advantage of the jacketed batch reactor design lies in its ability to precisely control the reaction temperature. This is realized through controlling the entering temperature and flow speed of a separate coolant stream circulating through the reactor jacket.

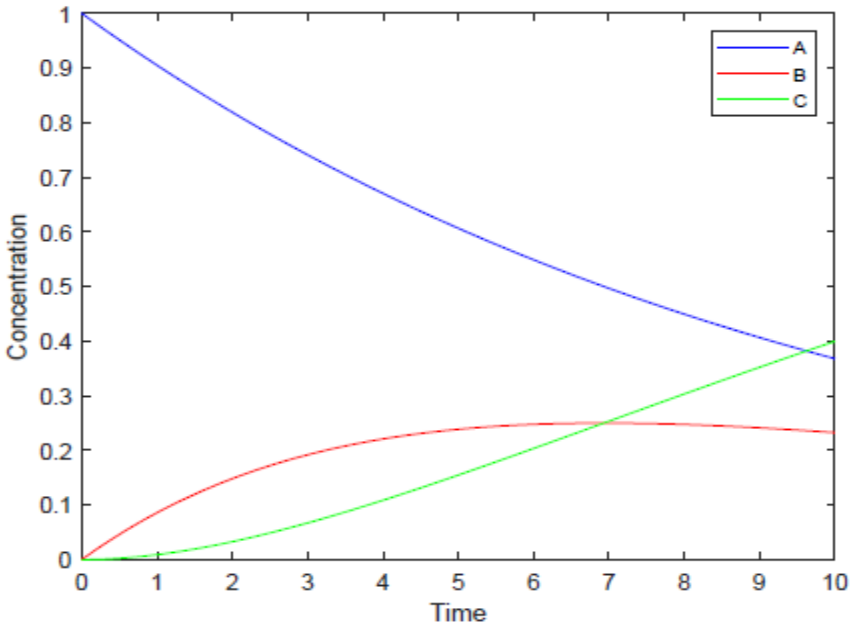

Figure 3.3 Concentration-time plot

Figure 3.3 depicts a concentration-time plot for three substances: A, B, and C. Substance A's concentration decreases over time, indicating it's a reactant being consumed in a chemical reaction. In contrast, substances B and C demonstrate increasing concentrations with a sigmoidal shape, suggesting they are products being formed. This pattern is consistent with a simple reaction where A transformed into B and C.

Precise temperature control is crucial for maximizing the formation of intermediate B, as reaction rates and product selectivity are highly sensitive to temperature variations. The generation of intermediary B can be increased by using this model. By predicting and optimizing operating conditions, it can achieve the desired high concentration of B. This involves connecting the ideas of reactant consumption, product formation, and reaction kinetics to understand how a system operates at a certain moment.

The changing behavior of the reaction process can be explained using a mathematical model that includes equations for the mass and energy balances.

The following assumptions were adopted for mathematical model development (Chen, 2014):

- Within the batch reactor, exothermic chemical processes take place.

- The reaction combination is well combined, the temperature and distribution of concentrations are both consistent. It is assumed that the volume, thermal conductivity, and density of liquid would remain constant. Shaft work-related energy dissipation is disregarded.
- Since the reactor is sealed, there isn't much heat exchange with the outside world.

The rate of reaction of A for a second order $A \rightarrow B$ is (Chen, 2014; Gilbert F. Froment et al., 2011):

$$r_A = -k_1(T)C_A{}^2, \quad C_A(0) = C_{A0} \tag{3.1}$$

where r_A is rate of reaction of A, k_1 is the rate constant for the conversion of A to B, C_A is a concentration of A and C_{A0} is the initial concentration of A. C_A at the time t=0 is C_{A0}. It indicates for the initial component A concentration that was charged into the reactor.

The reaction rate of B for first order $B \rightarrow C$ is (Chen, 2014; Gilbert F. Froment et al., 2011)

$$r_B = k_1(T)C_A{}^2 - k_2(T)C_B, \quad C_B(0) = 0 \tag{3.2}$$

where r_B is the rate of reaction of B, k_2 the rate constant for the conversion of B to C, C_B is concentration of B. At the onset of the reaction, product B is not present. Consequently, its initial concentration is set to zero.

The temperature-dependent reaction rates k_1 and k_2 are given by Arrhenius equations shown below (Chen, 2014)

$$k_1(T) = A_{10} \exp\left[-\frac{E_1}{RT}\right] \tag{3.3}$$

$$k_2(T) = A_{20} \exp\left[-\frac{E_2}{RT}\right] \tag{3.4}$$

where A_{10} and A_{20} are frequency factors of reaction A to B and B to C respectively. E_1 and E_2 are activation energies. R is gas constant.

3.2.1 Total Mass Balance Equation

According to the conservation of mass principle, the rate of a substance's buildup in a closed system equals the net inflow rate plus its generation rate from internal reactions (Gilbert F. Froment et al., 2011).

$$\begin{pmatrix} Rate\ of\ accumulation \\ within\ the\ system \end{pmatrix} = \begin{pmatrix} Net\ rate\ flow \\ into\ the\ system \end{pmatrix} + \begin{pmatrix} Rate\ of\ generation \\ by\ chemical\ reaction\ within\ the\ system \end{pmatrix}$$

The overall rate of flow into a system is the disparity between the amounts of flowing that enter and leave it.

$$\begin{pmatrix} Net\ rate\ of\ flow \\ into\ the\ system \end{pmatrix} = \begin{pmatrix} Rate\ of\ flow \\ into\ the\ system \end{pmatrix} - \begin{pmatrix} Rate\ of\ flow \\ out\ of\ the\ system \end{pmatrix}$$

$$F_n = F_{is} - F_{os}$$

where F_n is the net flow rate in to system, F_{is} and F_{os} are the flow rate into and out of the system respectively. Given a self-contained system with no inflow or outflow, the net rate of flow is zero. Additionally, due to mass conservation in chemical reactions, the rate of chemical reaction creation within the system is also zero. The rate at which mass changes in the system over time is expressed by (Conesa, 2020):

$$= \frac{dm}{dt}, m = \rho V \tag{3.5}$$

The time derivative of the system's mass (dm/dt) is estimated as the outcome of the liquid's density (ρ) and the reactor's volume (V).

Since density is constant;

$$\frac{d(\rho V)}{dt} = 0 \tag{3.6}$$

Consequently, the system's rate of mass accumulation is zero, as demonstrated by the preceding formula.

3.2.2 Component Balance Equation

The Batch process's component mass balance equation for reactant A at any instant time, *t* as follows (Conesa, 2020):

$$\begin{pmatrix} \textit{Flow} \text{ rate of A} \\ \text{into the reactor} \end{pmatrix} = \begin{pmatrix} \text{Flow rate of A} \\ \text{out of the reactor} \end{pmatrix} + \begin{pmatrix} \textit{Rate} \text{ of disapperance of A} \\ \text{by chemical reactor} \end{pmatrix} + \begin{pmatrix} \textit{Rate} \text{ of accumulation of A} \\ \text{within the reactor} \end{pmatrix}$$

In batch reactors, no fluid enters or leaves the reactor, hence

$$\begin{pmatrix} \textit{Net rate of flow} \\ \textit{into the system} \end{pmatrix} = \begin{pmatrix} \textit{Flow} \text{ rate of A} \\ \text{into the reactor} \end{pmatrix} - \begin{pmatrix} \text{Flow rate of A} \\ \text{out of the reactor} \end{pmatrix} = 0$$

The mass balance equation becomes

$$\begin{pmatrix} \textit{Rate} \text{ of accumulation of A} \\ \text{within the reactor} \end{pmatrix} = - \begin{pmatrix} \textit{Rate} \text{ of disapperance of A} \\ \text{by chemical reactor} \end{pmatrix}$$

Rate of accumulation of A signifies the net change in the amount of A within the reactor over time. A positive value indicates *A* is building up, while a negative value suggests it's being depleted. Since A is a reactant, its disappearance rate is always negative.

$$\text{Rate of disappearance of component } A = (-r_A)V \tag{3.7}$$

$$\text{Rate of generation of component } A = -(-r_A)V \tag{3.8}$$

$$\text{Rate of accumulation of component } A = \frac{dN_A}{dt} \tag{3.9}$$

where r_A is the rate of reaction of A and N_A is the number of moles of species A.

The time elapsed since the start of the process is

$$t = \frac{dN_A}{dt} = -(-r_A)V \tag{3.10}$$

The rate of accumulation of component A can be mathematically expressed as the time rate of change of N_A divided by the total volume of the reactor.

$$\frac{dN_A}{dt} = -(-r_A)V \tag{3.11}$$

Since V is constant

$$\frac{d(\frac{N_A}{V})}{dt} = -(-r_A), \ \frac{N_A}{V} = C_A$$
$$\frac{dC_A}{dt} = -(-r_A) \tag{3.12}$$

Since the reaction A to B is the second order kinetics (Chen, 2014)

$$(-r_A) = k_1(T){C_A}^2$$
$$\frac{d(C_A)}{dt} = -k_1(T){C_A}^2 \tag{3.13}$$

where C_A is the concentration of reactant A and k_1 is a rate constant for the conversion of A to B. This equation describes how the amount of substance A changes over time.

The following equation represents the component mass balance for reactant B within the batch reactor system. It allows tracking the rate of accumulation of B at any given time (t), which is solely determined by its consumption rate due to the ongoing chemical reaction.

$$\begin{pmatrix} Rate \text{ of accumulation} \\ \text{of component B} \end{pmatrix} = \begin{pmatrix} Net \text{ flow } rate \\ of \ component \text{ B} \end{pmatrix} + \begin{pmatrix} Rate \text{ of Generation} \\ \text{of Component B} \end{pmatrix}$$

$$\frac{dN_B}{dt} = 0 + r_B V \tag{3.14}$$

where N_B is represents the quantity of substance B in the system at a given point in time, V is the volume of the reactor and r_B is the speed at which B is being produced or consumed.

$$r_B = k_1(T){C_A}^2 - k_2(T)C_B$$
$$\frac{dC_B}{dt} = k_1(T){C_A}^2 - k_2(T)C_B \tag{3.15}$$

where C_B denotes the amount of the ingredient B in a particular amount of the reaction mixture and k_2 is a rate constant for the conversion of B to C. The component material balance for species B is represented in Equation (3.15).

3.2.3 Energy Balance Equation

This equation follows the principle of energy conservation and lead to the following formula is given:

$$\begin{pmatrix} Rate \text{ of energy} \\ \text{Accumulation} \end{pmatrix} = \begin{pmatrix} Net\ rate \text{ of energy} \\ \text{input} \end{pmatrix} + \begin{pmatrix} Rate\ of\ Energy \\ Generation \end{pmatrix}$$

Rate of energy accumulation represents the net change in the system's energy state. Positive value indicates the system is accumulating energy, while a negative value signifies energy is being lost. Net rate of energy input accounts for all the external energy entering the system. It could include heat added from a heating element, work done by a stirrer motor (although often negligible), or any other form of energy transfer from the environments.

$$\begin{pmatrix} Net \text{ rate of energy} \\ \text{input} \end{pmatrix} = \begin{pmatrix} Rate \text{ of heat input from} \\ \text{the heating jacket to the reactor} \end{pmatrix} - \begin{pmatrix} Rate \text{ of heat output from} \\ the \text{ reactor to the cooling coil} \end{pmatrix}$$

The heating jacket transfers heat to the reactor, while the cooling coil removes heat, with a coolant circulating to maintain the desired temperature (Chen, 2012).

$$= U_j A_j (T_s - T) - U_c A_c (T - T_c) \tag{3.16}$$

A_j, A_c are heat transfer areas, U_j, U_c are an overall heat transfer coefficient of heating and cooling coil respectively. T_s, T_c are steam and mean coil temperatures. Rate of energy generation specifically refers to the energy added (or removed) by the chemical reaction occurring within the reactor. For this term will be positive because the reaction releases heat, thereby adding energy to the system.

Energy production rate is influenced by both the reaction rate and the enthalpy change (ΔH) associated with:

$$\sum_{i=1}^{m} (-\Delta H_i)(r_i)V = (-\Delta H_1)k_1(T)C_A{}^2V + (-\Delta H_2)k_2(T)C_BV \tag{3.17}$$

where ΔH_i is the enthalpy over a particular component, r_i is rate of reaction and m is number of components. Heat is being transferred out of the system, as indicated by the negative value.

The derivative of the system's total energy with respect to time is accumulation rate given by:

$$\begin{aligned}\frac{dE}{dt} &= \frac{d(V\rho h)}{dt}, h = C_p T \\ &= \rho V C_p \frac{dT}{dt}\end{aligned} \tag{3.18}$$

where ρ the density of reactor mixture and enthalpy h represents the total heat a system possesses at a fixed pressure. It's a property that's determined by the system's beginning and ending points. C_p is Specific heat capacity.

When we rearrange the above equations (Chen, 2012)

$$\begin{aligned}\rho V C_p \frac{dT}{dt} &= (-\Delta H_1) k_1 {C_A}^2 V + (-\Delta H_2) k_2 C_B V + U_j A_j (T_s - T) - U_c A_c (T - T_c) \\ \frac{dT}{dt} &= \frac{(-\Delta H_1) k_1 {C_A}^2 V}{\rho V C_p} + \frac{(-\Delta H_2) k_2 C_B V}{\rho V C_p} + \frac{U_j A_j}{\rho V C_p}(T_s - T) - \frac{U_c A_c}{\rho V C_p}(T - T_c)\end{aligned} \tag{3.19}$$

3.3 Dimensionless of the Batch Process Parameters

Dimensionless parameters offer a powerful tool for batch reactor modeling. They simplify complex models by reducing independent variables, making them easier to analyze. This newfound clarity allows for comparisons across different reactor sizes and operating conditions, facilitating the crucial step of scaling up from lab experiments to industrial applications. More importantly, these dimensionless groups act as spotlights, highlighting the key factors that truly influence the reactor's performance, allowing engineers to focus their efforts on optimizing the most impactful parameters.

A temperature trajectory designed to maximize component *B* yield in a batch reactor with a one-hour operation time. This trajectory dictates how the temperature should change over the course of the reaction to achieve the highest possible production of component *B* within that one-hour timeframe (Ray & Szekely, 1973).

$$T_d(t) = 54 + 71\exp(-25\times10^{-3}t) \tag{3.20}$$

where T_d is the desired temperature. Therefore, the control strategy aims to make the batch reactor closely follow the optimal temperature trajectory identified (Ray & Szekely, 1973).

To ensure precise temperature control, the system must be capable of both heating and cooling the reactor as needed. Steam pressure controls heating, while coolant flow regulates cooling, affecting overall heat transfer.

With the coolant flow rate (F_c) and the overall heat transfer coefficient (U_c), a correlation is shown as (Ravi, 2017)

$$\frac{1}{U_c} = \frac{1}{4550 F_c^{0.8}} + \frac{1}{10.8} \tag{3.21}$$

The simultaneous use of heating and cooling in a batch reactor results in too many constraints in system, meaning there are more control quantities (steam pressure and coolant flow rate) than necessary to achieve a single objective (temperature). To address this, (Jutan & Uppal, 1984) propose a simplified approach. They present just one variable, denoted by *u*, which encompasses both manipulated variables simultaneously.

$$T_s = (T_{s,\max} - T_{s,\min})u + T_{s,\min} \tag{3.22}$$

$$U_c = (U_{c,\min} - U_{c,\max})u + U_{c,\max} \tag{3.23}$$

The highest and lowest values for both steam pressure (T_s) and overall heat transfer coefficient (U_c) are chosen based on process limitations and safety constraints. This ensures safe and efficient operation. A single parametric variable, *u*, is then introduced, encompassing both T_s and U_c. By manipulating *u*, the control system can determine the heating and cooling rates simultaneously for precise temperature tracking. Substituting Equations (3.22) and (3.23) into Equation (3.19) followed by rearrangement will yield the control law for the batch reactor as follow:

$$\frac{dT}{dt} = \gamma_1 k_1(T) C_A{}^2 + \gamma_2 k_2(T) C_B + (\alpha_1 + \alpha_2 T) + (\beta_1 + \beta_2 T)u \tag{3.24a}$$

where

$$\gamma_1 = \frac{(-\Delta H_1)}{\rho C_p} \tag{3.24b}$$

$$\gamma_2 = \frac{(-\Delta H_2)}{\rho C_p} \tag{3.24c}$$

$$\alpha_1 = (U_j A_j T_{s,\min} + U_{c,\max} A_c T_c) / \rho C_p V \tag{3.24d}$$

$$\alpha_2 = -(U_j A_j + U_{c,\max} A_c) / \rho C_p V \tag{3.24e}$$

$$\beta_1 = [U_j A_j (T_{s,\max} - T_{s,\min}) - (U_{c,\max} - U_{c,\min}) A_c T_c] / \rho C_p V \tag{3.24f}$$

and

$$\beta_2 = (U_{c,\max} - U_{c,\min}) A_c] / \rho C_p V \tag{3.24g}$$

The system of differential equations composed of Equations (3.13), (3.15), and (3.24a) represents a mathematical model for a batch reactor process. *u* is dimensionless (unitless) and normalized between 0 and 1. At *u*=0, the system experiences maximum cooling and minimal heating, while *u*= 1 signifies the opposite. This simplifies the control problem. The goal is now to identify a value for *u* between 0 and 1 that ensures the batch reactor's temperature closely follows the target profile, even when faced with disturbances or uncertainties.

3.4 Dynamic Analysis of a Batch Reactor Process

The complex and dynamic nature of batch reactors present significant challenges in achieving optimal performance, product quality, and safety. Traditional modeling approaches often fall short in capturing the intricate interactions between process variables and the time-dependent behavior of batch reactors (Niu & Yang, 2013).

Dynamic analysis provides a powerful framework for investigating the evolution of a batch process over time. (Podofillini & Dang, 2012) By employing mathematical models that describe the system's rate of variation, it is possible to gain valuable insights into the factors influencing product yield, quality, and process efficiency.

3.4.1 State Space Modeling for a Batch Reactor Process

The changes in a batch reactor over time can be described using a series of first-order differential equations. These equations form a state space model that connects inputs and outputs. Let the state variables of the dimensionless concentrations and temperature $x_1=C_A$, $x_2=C_B$ and $x_3=T$, then the state equations are given by

$$\dot{x}_1 = -k_1(T) x_1^2 \tag{3.25a}$$

$$\dot{x}_2 = -k_1(T) x_1^2 - k_2(T) x_2 \tag{3.25b}$$

$$\dot{x}_3 = \gamma_1 k_1(T) x_1^2 + \gamma_2 k_2(T) x_2 + (\alpha_1 + \alpha_2 x_3) + (\beta_1 + \beta_2 x_3) u \tag{3.25c}$$

Since Equation (3.25) is a nonlinear system in which the control appears linearly, it is called an input-affine. It is expressed by the vector differential equation as

$$\dot{\boldsymbol{x}} = \boldsymbol{f}(\boldsymbol{x}) + \boldsymbol{g}(\boldsymbol{x}) u \tag{3.26}$$

where $\boldsymbol{x} = [x_1\ x_2\ x_3]^T \in \Re^3$ is the state vector, $\boldsymbol{f}(\boldsymbol{x})$ and $\boldsymbol{g}(\boldsymbol{x})$ are the nonlinear vector functions defined as

$$\boldsymbol{f}(\boldsymbol{x}) = \begin{bmatrix} -k_1(T) x_1^2 \\ -k_1(T) x_1^2 - k_2(T) x_2 \\ \gamma_1 k_1(T) x_1^2 + \gamma_2 k_2(T) x_2 + (\alpha_1 + \alpha_2 x_3) \end{bmatrix} \tag{3.27}$$

$$\boldsymbol{g}(\boldsymbol{x}) = \begin{bmatrix} 0 \\ 0 \\ \beta_1 + \beta_2 x_3 \end{bmatrix} u \tag{3.28}$$

3.4.2 Open-loop Analysis of a Batch Reactor Process

Understanding batch behavior is crucial for optimizing reaction yields, conversion rates, and overall process efficiency. An open-loop analysis provides a fundamental approach to predicting the dynamic behavior of the reactor system without relying on any feedback control mechanisms. This analysis helps to establish a baseline understanding of the relationship between initial conditions, reaction kinetics, and the resulting concentration and temperature profiles within the reactor over time. The insights gained from this analysis serve as a foundation for further exploration of control strategies that can be implemented to achieve desired reactor performance.

3.4.3 Equilibrium State

Although batch reactors are inherently dynamic, elements of steady-state analysis can provide valuable insights. By examining the relationship between a key component's concentration and reaction time, we can gain a preliminary understanding of system behavior. However, it's crucial to remember that batch reactors never achieve a true steady state due to their continuously changing conditions.

While batch reactors operate dynamically, steady-state concepts can be leveraged for simplified modeling and initial analysis. By creating models based on steady-state assumptions, we can capture essential process characteristics, aiding in parameter estimation and control system design. Nonetheless, these models are approximations and must be complemented by dynamic analysis for a comprehensive understanding of reactor behavior.

Equilibrium analysis in batch reactors focuses on determining the final composition of the system when the reaction has ceased progressing. (Scott Fogler, 2016) This involves solving the equilibrium equations, which are derived from the stoichiometry of the reaction and the equilibrium constant.

Unlike continuous stirred-tank reactors (CSTRs), which can operate at stable equilibrium points under specific conditions, batch reactors are inherently dynamic systems without such equilibrium states. Batch processes undergo deliberate changes in state variables over time, aiming for a desired final state or target condition rather than a constant equilibrium. Equilibrium points, characterized by unchanging system properties, are determined by solving the state space equations with zero inputs for systems with such behavior.

To find the equilibrium point, it is imperative to resolve the system of equations for the state variables by setting their derivatives to zero. As shown in Equation (3.25), letting $\dot{x}_1 = 0$, $\dot{x}_2 = 0$ and $\dot{x}_3 = 0$ leads to

$$0 = -k_1(T)x_1^2 \tag{3.26a}$$

$$0 = k_1(T)x_1^2 - k_2(T)x_2 \tag{3.26b}$$

$$0 = \gamma_1 k_1(T)x_1^2 + \gamma_2 k_2(T)x_2 + (\alpha_1 + \alpha_2 x_3) + (\beta_1 + \beta_2 x_3)u \tag{3.26c}$$

Since $k_1(T)$ and $k_2(T)$ are a non-zero constant, the only values of x_1 and x_2 that satisfies Equations (3.26a) and (3.26b) are $x_1 = 0$ and $x_2 = 0$. Substituting $x_1 = 0$ and $x_2 = 0$ into Equation (3.26c), the control input in the equilibrium state becomes

$$u = -\frac{\alpha_1 + \alpha_2 x_3}{\beta_1 + \beta_2 x_3} \tag{3.27}$$

The goal is to develop a control input that u, constrained between 0 and 1, that enables the batch reactor temperature to accurately follow a specified, wide-range temperature trajectory. The purpose must be met even in the face of unexpected events and inaccuracies in the system model.

CHAPTER FOUR

DESIGN OF A TDOF NPID CONTROLLER FOR A BATCH REACTOR PROCESS

This chapter explores the development and refinement of a TDOF NPID controller for a batch reactor process. First, we examine the existing linear and nonlinear PID controllers to provide the theoretical background for designing the proposed controller and for performance comparison purposes. The core objective lies in establishing a systematic approach for optimizing the controller's parameters to achieve desired performance objectives in the batch reactor system. PSO is employed to find the best settings for the controllers.

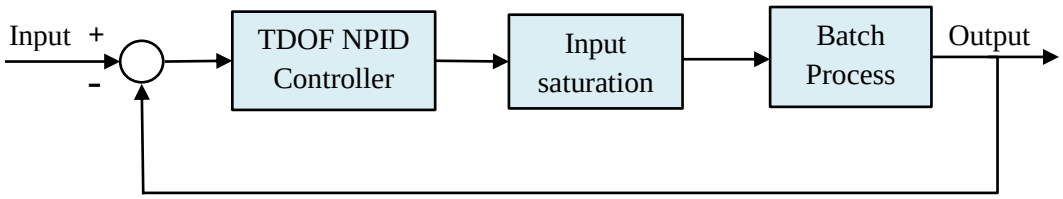

Figure 4.1 Structure of the proposed Batch Reactor temperature control system

4.1 Existing Linear and Nonlinear Controllers

4.1.1 Linear PID Controller

A PID controller is a versatile control loop mechanism that measures the difference between the desired value and the actual value and adjusts the system accordingly. (Oliveira et al., 2014). It then applies a correction comprising three components: proportional, integral, and derivative. They are prevalent in control systems due to their simplicity and effectiveness. They have been widely applied in various industries, from process control to robotics.

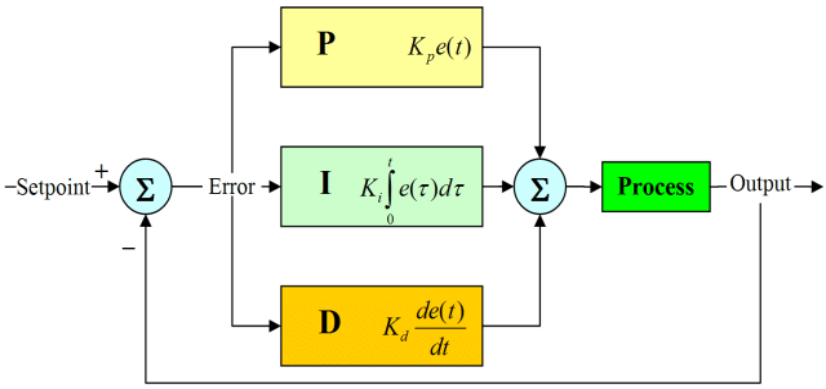

Figure 4.2 Schematic diagram of the PID controller (Halim & Ismail, 2019)

(Borase et al., 2021) PID controllers combine proportional, integral, and derivative control actions to regulate processes. The proportional term corrects current errors, while the integral term eliminates steady-state error by accumulating past errors. The derivative term improves transient response by anticipating future error changes. However, the derivative term can amplify high-frequency noise or sudden setpoint changes, causing a phenomenon known as *derivative kick*. Filtering techniques are often employed to mitigate this issue and enhance overall control performance. One type of controller that incorporates a first-order filter is the practical PID controller, a prevalent control algorithm in various industrial applications, from process control to robotics.

The following formula characterizes the frequency domain behavior of the PID controller:

$$G_{pid}(s) = K_p + \frac{K_i}{s} + K_d D(s) \tag{4.1a}$$

$$D(s) = \frac{s}{1 + \frac{T_d}{N} s} \tag{4.1b}$$

where K_p, K_i and K_d are the proportional, integral, derivative gains, respectively. $T_d = K_d/K_p$ denotes the derivative time. $D(s)$ is an approximation of the ideal differentiator and N is a user-defined parameter.

The derivative term in a PID controller, while enhancing system response by anticipating error changes, is susceptible to high-frequency noise amplification due to its differentiation function. This heightened sensitivity to rapid fluctuations results in an increased noise-to-signal ratio, potentially destabilizing the control system and degrading performance. Consequently, filtering techniques are often employed to attenuate these high-frequency components, preserving the derivative term's benefits while mitigating its adverse effects on

system stability and accuracy.

The magnitude of its frequency is

$$K_d \mid D(j\omega) \mid = K_d\omega / \sqrt{1+T_d^2\omega^2 / N^2} \tag{4.2}$$

where $D(j\omega)$ is the frequency domain representation of the derivative filter, $|D(j\omega)|$ is shows how much the filter amplifies or attenuates different frequencies, and ω is represents the angular frequency.

The equation shows that the magnitude of the derivative filter's output is a function of input frequency (ω) and derivative gain (K_d). However, this output is also influenced by the denominator term, which acts as a low-pass filter. As ω increases, the denominator term grows larger, reducing the overall magnitude of the filter's output. This means that high-frequency components of the input signal will be attenuated, while lower frequency components will pass through with a greater impact. In essence, the equation describes how the derivative filter amplifies high-frequency signals to a limited extent while significantly reducing the impact of low-frequency components.

As the frequency increases, the denominator of the filter's transfer function becomes dominated by the $T_d\omega/N$ term. The filter's magnitude eventually stabilizes at a value of NK_d/T_d. However, this value is capped at NK_p as the frequency increases infinitely. This implies that high-frequency noise is amplified by a maximum factor of NK_p. To achieve the desired filtering effect, N is set to a value between 5 and 30. (O'dwyer A., 2009). Note that if $N \to \infty$, $D(s)$ becomes the ideal differentiator.

Figure 4.2 depicts the PID control system, where y_s denotes the set-point, y the outcome, e the error deviation from set-point, d the disturbance, u the control input, u_{sat} the saturated control input, and $Sat(u)$ the saturation defined as

$$u_{sat}(t) = \begin{cases} 1, & u(t) > 1 \\ u(t), & 0 \le u(t) \le 1 \\ 0, & u(t) < 0 \end{cases} \tag{4.3}$$

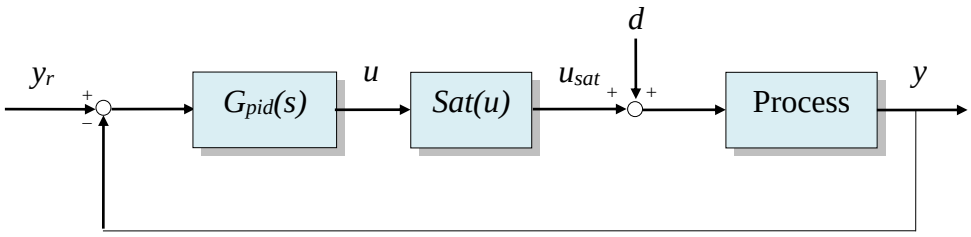

Figure 4.3 The PID control system.

4.1.2 Nonlinear PID Controller

Linear PID controllers guarantee good performance when they are operated near the designed region. However, as the process dynamics change or become unpredictable, their performance may degrade significantly. Traditional PID control methods often struggle to balance rapid response with minimal overshoot, resulting in suboptimal performance. (H. Zhang & Hu, 2012).

For processes with nonlinear characteristics like this, one alternative is to use NPID controllers that offer several advantages, such as reduced overshoot and oscillation and improved robustness to disturbances in a variety of applications (Korotkin et al., 2010).

Compared to these advantages, the structures of NPID controllers are more complex to design and implement than those of linear PID controllers and their tuning parameters also increase. Recently, NPID controllers are becoming increasingly popular in research community (Su et al., 2005). (Jin & Son, 2019) proposed the NPID controller, a simpler alternative to traditional PID controllers, uses a nonlinear gain with the integral term. This allows for better transient response when errors are large by adjusting the gain accordingly. Conversely, when the error is negligible, a higher nonlinear gain can quickly eliminate offset. This dynamic adjustment of the nonlinear gain is crucial to balance both stability and accuracy.

We use this NPID controller and its control law expressed as

$$\begin{aligned} u(t) &= u_p(t) + u_i(t) + u_d(t) \\ u_p(t) &= K_p e(t) \\ u_i(t) &= K_i \int v(t)dt \\ \frac{T_d}{N}\frac{du_d(t)}{dt} + u_d(t) &= K_d \frac{de(t)}{dt} \end{aligned} \tag{4.4}$$

where u_p, u_i and u_d denote the proportional, integral and derivative actions, respectively and the gains are the same as used in the linear PID controller. $v(t)$ is the scaled error that is given by

$$v(t) = k(e)e(t) \tag{4.5}$$

$k(e)$ in Equation (4.5) is a nonlinear gain defined by

$$k(e) = \exp(-\frac{e^2}{2\sigma^2}) \tag{4.6}$$

where σ represents the greatest difference in the step-type setpoint's current value from its prior value.

Figure 4.3 shows the graphical representation of $v(t)$ for typical values of σ= 1.5, 1.0 and 0.5. The figure demonstrates that the nonlinear function *k(e)* effectively mitigates excessive control effort during significant setpoint changes or disturbances by scaling down the error. This property contributes to improved transient response.

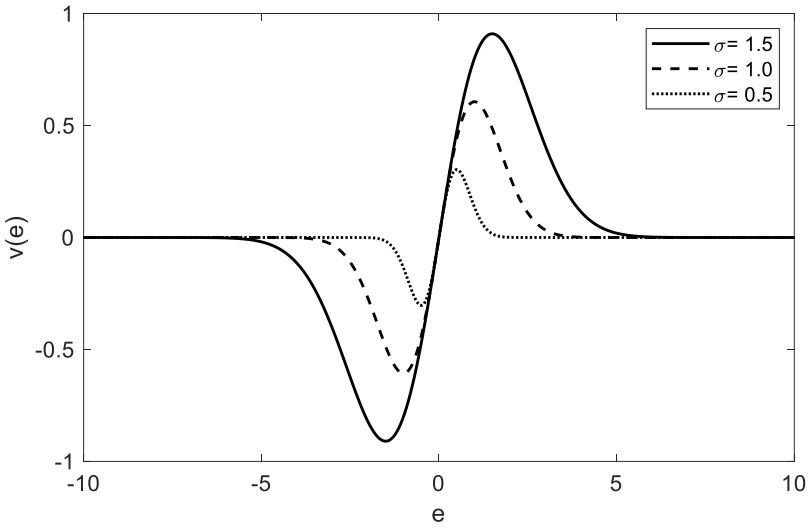

Figure 4.4 Graphical representation of v(t) for typical values of σ = 1.5, 1.0 and 0.5.

The frequency-domain illustration of the linear part of the NPID controller and the process yields the following relationship.

$$G_{pd}(s) = \frac{U_{pd}(s)}{E(s)} = K_p + K_d D(s), \tag{4.7a}$$

$$\frac{U_i(s)}{V(s)} = \frac{K_i}{s} \tag{4.7b}$$

where *D(s)* remains unchanged from Equation (4.1b).

System control of NPID can be observed in Figure 4.4. The desired value is y_s, the actual value is *y*, the control action is *u*, the difference between the desired and actual values is *e*, and the scaled error is *v*.

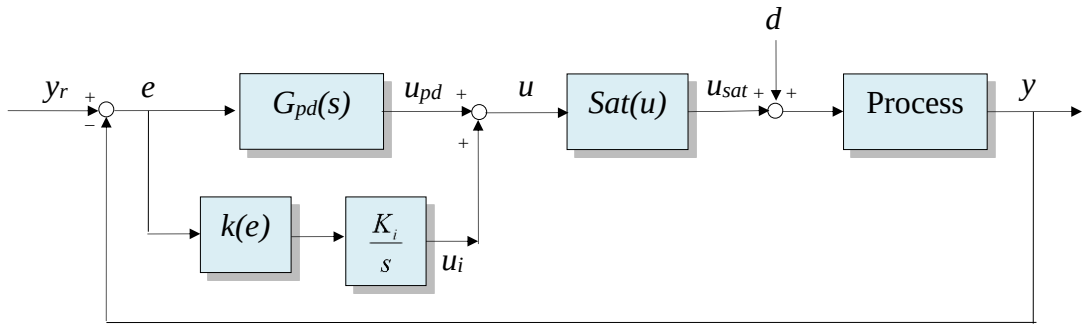

Figure 4.5 The NPID control system

While the previously mentioned NPID controller offers advantages over the linear PID controller, it remains a one-degree-of-freedom (ODOF) controller. This inherent limitation restricts its ability to perfectly balance improvements in both setpoint tracking and disturbance rejection.

4.2 Design of a TDOF NPID Controller

A control system's flexibility is determined by the number of independently adjustable closed-loop behaviors. Two-degree-of-freedom systems offer greater design freedom than their ODOF counterparts due to the complex nature of control system objectives (Araki & Taguchi, 2003). This section introduces a new controller that employs the TDOF and NPID techniques.

4.2.1 NPID controller with a PD-type feedforward compensator

As mentioned before, one of the limitations of conventional ODOF PID controllers is that they cannot simultaneously improve the desired output value while mitigating external influences. Improving setpoint tracking capability worsens disturbance rejection capability, and vice versa. However, there are ways to mitigate this limitation by using adaptive control or introducing TDOF control in a feedforward or feedback path. One of popular choices for

industrial applications is the use of TDOF control in a feedforward path. It proposes TDOF NPID control scheme with a feedforward compensator as shown in Figure 4.5.

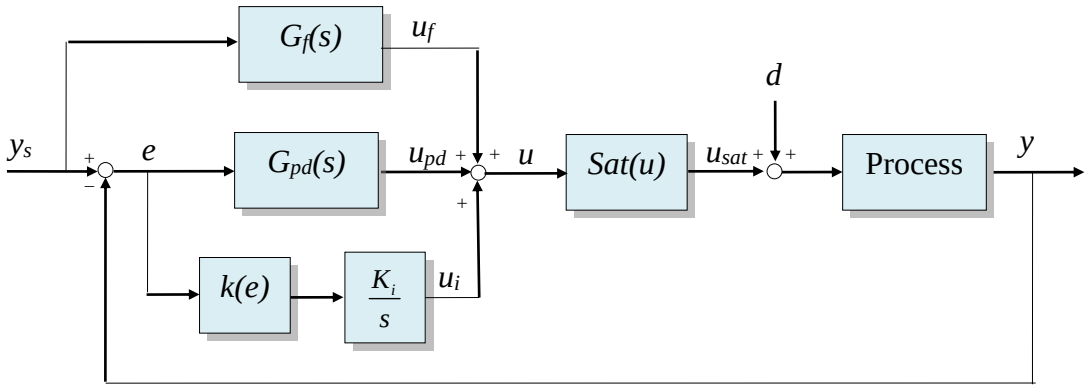

Figure 4.6 TDOF NPID control system with a feedforward compensator u_f

A PD-type of the feedforward compensator is the form proposed by (Araki, 1984) as

$$G_f(s) = -K_p[\alpha + \beta T_d D(s)] \tag{4.8}$$

where α and β are the setpoint weight on proportional term and derivative term, respectively. $D(s)$ is the same as in Equation (4.1b). The TDOF NPID controller in Figure 4.5 can overcome the limitations of ODOF linear or nonlinear PID controllers by providing one additional degree of freedom which allows for more flexibility in tuning the controller.

From the Figure 4.5, we have the following expressions

$$\begin{aligned} U_{pd}(s) &= G_{pd}(s)E(s) \\ E(s) &= Y_s(s) - Y(s) \end{aligned} \tag{4.9a}$$

$$U_f(s) = G_f(s)Y_s(s) \tag{4.9b}$$

Combining the Equations (4.7a), (4.8) and (4.9), the linear parts of the TDOF NPID controller can be written as

$$\begin{aligned} U_{pd}(s) + U_f(s) &= G_{pd}(s)E(s) + G_f(s)Y_s(s) \\ &= K_p[1 + T_d D(s)][Y_s(s) - Y(s)] - K_p[\alpha + \beta T_d D(s)]Y_s(s) \\ &= K_p[(1-\alpha)Y_s(s) - Y(s)] + K_p T_d D(s)[(1-\beta)Y_s(s) - Y(s)] \end{aligned} \tag{4.10}$$

Then, the equivalent block diagram is redrawn as in Figure 4.6.

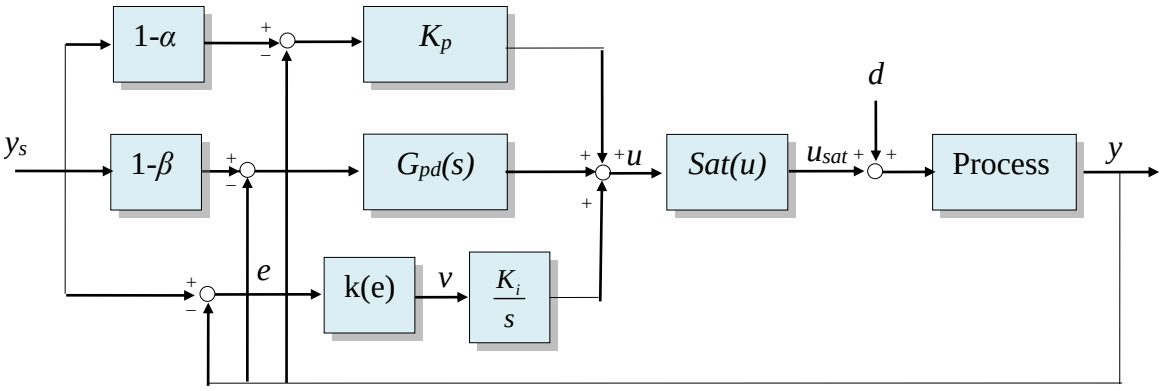

Figure 4.7 Equivalent TDOF NPID control system.

This controller offers five parameters (K_p, K_i, K_d, α, β) that can be adjusted to tune its behavior.

4.4 Optimal Tuning of the TDOF NPID Controller

Precise temperature control is paramount for achieving optimal product quality in batch reactors. While traditional PID controllers suffice for many processes, the inherent complexities and nonlinearities of these systems often necessitate more advanced control strategies. While the TDOF NPID controller can potentially enhance a system's ability to handle complex process dynamics by combining PID control with a nonlinear element, its performance may vary depending on specific applications.

A TDOF NPID controller uses two separate control mechanisms: servo control for quickly reducing errors and regulatory control for eliminating steady-state offsets. This dual-action approach can provide benefits in managing the complexities of batch processes, but its effectiveness may vary depending on specific applications. To fully harness the potential of the TDOF NPID controller, meticulous parameter tuning is essential. By carefully adjusting proportional (K_p), integral (K_i), and derivative (K_d) gains, engineers can optimize product quality, process efficiency, and system robustness.

Effective controller tuning is essential for optimizing controller performance, ensuring system stability, achieving precise tracking of setpoints, maximizing efficiency, and maintaining robustness in the face of operational disturbances. This study uses PSO for tuning the parameters of controllers.

4.4.1 PSO algorithm as an optimization tool

PSO is computational intelligence method was motivated by the group dynamics of bird flocking. A swarm of particles repeatedly looks for the best output in this population-based optimization technique. Based on both its own most well-known position (*pbest*) and the most prevalent position of the entire swarm (*gbest*), each particle is a candidate solution.

Each particle in a PSO swarm maintains a personal best (*pbest*) position, representing its best solution encountered thus far. This information guides a particle's exploration of the search space. Additionally, the swarm collectively tracks the global best (*gbest*) position, the overall best solution found, and fostering knowledge sharing among particles and encouraging movement towards promising regions.

The key concept of PSO resides in the dynamic update of particle velocities. This velocity term introduces momentum, allowing particles to explore new regions while maintaining a connection to previously explored areas. The combination of *pBest* and *gBest* information within the velocity update equation steers particle movement towards promising regions with the potential to lead to even better solutions.

One of the significant advantages of PSO lies in its simplicity. It requires minimal parameter tuning compared to other optimization methods, making it readily applicable to diverse problems. Additionally, PSO demonstrates efficient convergence, often finding good solutions within a reasonable timeframe, particularly for continuous optimization problems. These advantages, coupled with its intuitive nature, have propelled PSO to become a popular choice for a wide range of optimization tasks across various disciplines. From engineering design optimization to machine learning, robotics control, and financial modeling, PSO continues to offer a robust and efficient approach for unearthing optimal solutions in complex problem domains.

PSO Initialization involves defining the optimization problem, setting parameters, and creating an initial population of particles. The problem definition includes the objective function and constraints. Parameters such as population size, search space boundaries, inertia weight, and learning rates are established. Particles are randomly positioned within the search space, and their initial fitness values are calculated.

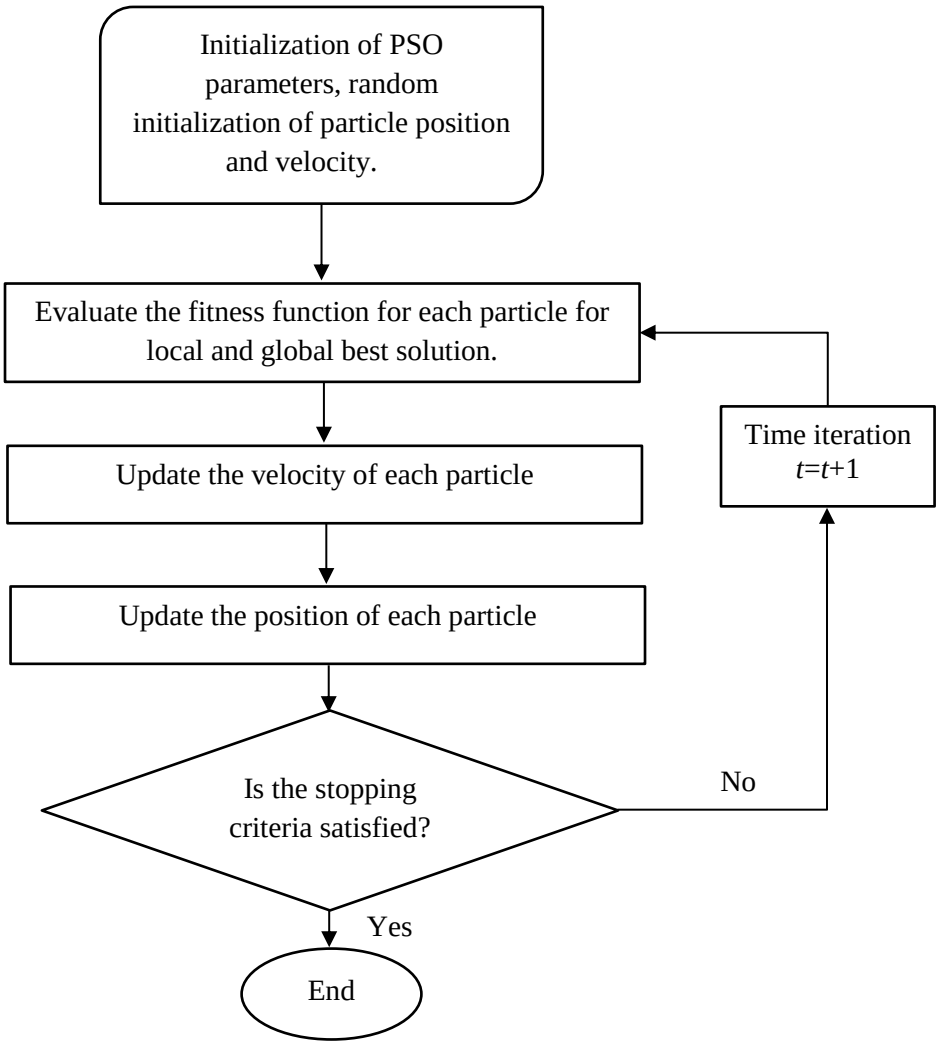

Figure 4.8 Flow chart of PSO algorithm

The iterative optimization process involves updating particle positions based on their fitness values. The global best (gBest) for each particle is determined through contrasting the personal best (pBest) to the present fitness. Particle velocities are adjusted based on *pBest*, *gBest*, and previous velocity, influencing the direction and magnitude of movement. New particle positions are calculated and evaluated, with the process repeating until a termination condition is met.

Once a predetermined stopping condition is satisfied, such as reaching the highest number of cycles or arriving at a workable solution, the PSO algorithm comes to an end. The best particle found within the swarm represents the optimized solution. While specific PSO implementations may vary in velocity updates, parameter tuning, and particle interactions, the core principles of *pBest*, *gBest*, and iterative search remain fundamental to the algorithm.

Velocity Update Equation is

$$v\_id(t+1) = w*v\_id(t) + c1*rand1*[pbest\_id(t) - x\_id(t)] + c2*rand2*[gbest(t) - x\_id(t)] \quad (4.11)$$

where *w* is the inertia weight (which regulates momentum), *v_id(t)* is the velocity of particle i at iteration t, and *v_id*(*t*-1) is the velocity of particle i at previous iteration (*t*-1), *pbest_id(t)* is the best position found by particle *i* up to iteration t (personal best), *c2* is the social learning coefficient, *rand2* is a random number between 0 and 1, *gbest(t)* is the best position found by the entire swarm up to iteration *t* (global best), *x_id(t)* is the current position of particle *i* at iteration *t*, and *c1* is the cognitive learning coefficient.

The position update equation determines the computed velocities, which are used by the particles to modify their positions inside the field of search.

$$x\_id(t+1) = x\_id(t) + v\_id(t+1) \quad (4.12)$$

x_id(t) and *x_id(t+1)* denote the locations of particle *i* at iterations *t* and *t*+1.For the upcoming version, this update establishes each particle's new placement within the search space. Particle locations and velocities are iteratively updated by the PSO algorithm using data from the global best (*gBest*) and personal best (*pBest*) sets. This process keeps on until a termination condition is satisfied, like finishing the most iterations or coming up with a workable solution. Particles gradually converge to the best area within the search space.

The principal aim of employing PSO in this study is to optimize the TDOF NPID controller parameters (K_p, K_i, K_d, α and β) to achieve optimal performance of the batch reactor temperature control system across its entire operating range.

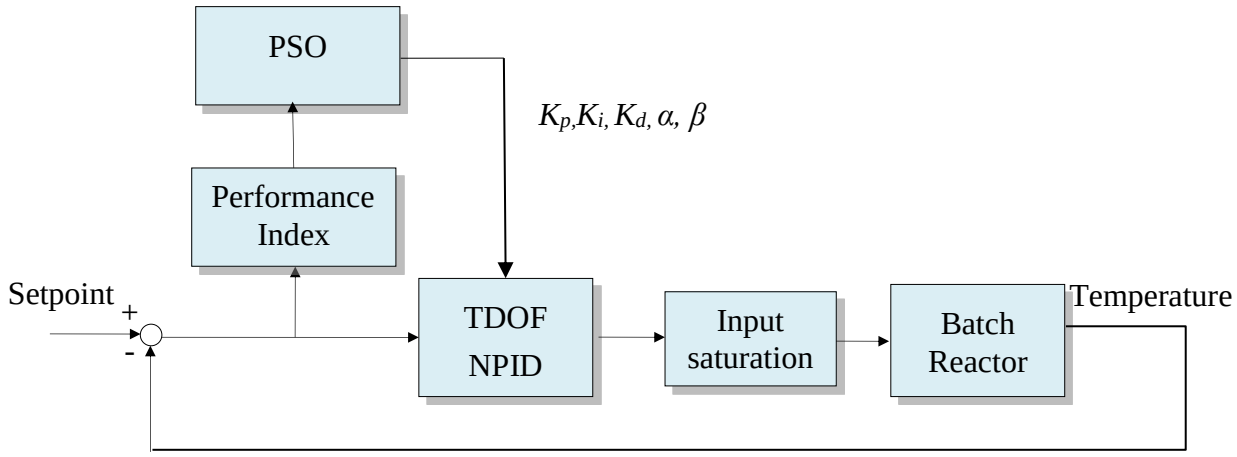

Figure 4.9 TDOF NPID controller tuning using PSO

4.4.2 Performance Indices

Performance indices are quantitative measures used to assess how good a control system's response to a given input. They provide a numerical basis for comparing different control strategies and tuning parameters (Almabrok et al., 2018). Control system performance can be measured using various performance indices, such as integral absolute error (IAE), integral square error (ISE), integral of time absolute error (ITAE), and integral of time square error (ITSE) (Mishra et al., 2014) .

Integral Square Error (ISE):

$$ISE = \int e^2 dt \tag{4.13}$$

Integral Absolute Error (IAE):

$$IAE = \int |e| \, dt \tag{4.14}$$

Integral of Time Absolute Error (ITAE):

$$ITAE = \int t \, |e| \, dt \tag{4.15}$$

Integral of Time Squared Error (ITSE):

$$ITSE = \int te^2 dt \tag{4.16}$$

where *e* represents the discrepancy between the desired value and the actual value.

ISE prioritizes rapid error reduction, often leading to oscillatory responses. Conversely, IAE emphasizes overall error minimization, resulting in slower but smoother responses. ITAE balances these two objectives by penalizing errors that persist over time, promoting faster settling without excessive oscillation. ITSE, a variant of ITAE, places a heavier emphasis on minimizing the error's impact over time, potentially leading to even faster settling but potentially at the cost of increased initial response. The proposed control system's performance is evaluated using IAE, which measures the overall deviation of the controlled response from the desired setpoint. By minimizing it, the system effectively rejects disturbances and ensures a stable and accurate process.

Another performance index is Integral Absolute Error and Control Signal (IAEU) that combines both the system error and control effort into a single metric. It is calculated by integrating the absolute value of the error and the absolute value of the control signal over a specific time period (Shuaib & Ahmed, 2014).

$$IAEU = \int_0^\infty |e(t)| + w|\Delta u(t)|\,dt \tag{4.18}$$

where $e(t)$ is the error, with $e(t)= y_s-y(t)$, $u(t)$ is the deviation of the control input with $\Delta u(t)= u(t)-u_0$, and w is the weighting factor.

For u_0, Equation (3.26c) is used. The weighting factor, w, balances the relative importance of system error and control effort components. A w value of one equally considers error and control effort, while values greater than one prioritize control effort and values less than one emphasize error reduction. Setting w to zero reduces IAEU to the traditional IAE, neglecting control effort altogether. Because it can account for both process error and control effort, IAEU is an adequate performance index for maintaining temperatures in batch reactors. By incorporating energy efficiency and actuator protection into the evaluation, IAEU helps to optimize system performance.

CHAPTER FIVE

SIMULATION RESULT AND DISCUSSION

The PSO-tuned TDOF NPID controller is assessed in this chapter using the chemical batch reactor's nonlinear model. Both the PID controller in Figure 4.2 and the NPID controller in Figure 4.4 are implemented for comparison. PSO tunes the NPID controller, and the Tyreus-Luyben technique tunes the PID controller. Based on rejection of disturbances and setpoint tracking, the three controllers are evaluated. The setpoint tracking achievements is evaluated based on how quickly (swiftness) and accurately (closeness) the system responds to changes in the desired temperature setpoint. Closeness describes how closely the output matches the setpoint, whereas swiftness describes the output's capacity to track changes in the setpoint quickly. They are assessed by some metrics such as overshoot (M_p) and settling time (t_s). To assess the overall performance of the three controllers, one measure in terms of IAE is employed.

$$IAE = \int_0^\infty | y_s(t) - y(t) | dt \tag{5.1}$$

where y_s is the setpoint and y is the output.

5.1 Parameters of the Batch Reactor

The summary of variables used for the batch reactor process model with their value is listed below.

Table 5.1 Process parameters and values (Chen, 2014)

Parameter	Description	Value	Unit
A_{10}	Reaction A to B's frequency factor	1.1	$m^{3}.kmol^{-1}.s^{-1}$
A_{20}	Reaction B to C's frequency factor	172.2	s^{-1}
E_1	Activation energy 1	20900	$KJ.kg^{-1}.K^{-1}$
E_2	Activation energy 2	41800	$KJ.kg^{-1}.K^{-1}$
R	Gas Constant	8.3143	$KJ.kmol^{-1}.K^{-1}$
T_c	Current temperature of reactor	25	°C
$T_{s,max}$	Maximum allowable temperature setpoint	150	°C
$U_{c,max}$	Maximum allowable overall heat transfer coefficient	4.42	$KJ.m^{-2}.°C^{-1}.s^{-1}$
γ_1	Ratio of specific heats 1	41.8	$°C.s^{-1}$
γ_2	Ratio of specific heats 2	86.6	$°C.s^{-1}$
α_1	Rate of heat transfer 1	4.3145	$°C.s^{-1}$
α_2	Rate of heat transfer 2	-0.1099	$°C.s^{-1}$
β_1	Intensity of heat transmission 1	1.4962	$°C.s^{-1}$
β_2	Intensity of heat transmission 2	0.0515	$°C.s^{-1}$
$T_{s,min}$	Minimum allowable temperature setpoint.	70	°C
$U_{c,min}$	Minimum allowable overall heat transfer coefficient	1.39	$°C.s^{-1}$

The initial conditions of concentration of A, concentration of B and temperature used in the nonlinear model of Equation (3.25) are as follows:

$$C_A(0)= x_1(0)= 1\ kmol.m^{-1} \tag{5.2a}$$

$$C_B(0)= x_2(0)= 0\ kmol.m^{-1} \tag{5.2b}$$

$$T(0)= x_3(0)= 25°C \tag{5.2c}$$

5.2 Controller Parameter Settings

The NPID and TDOF-NPID controllers are adjusted in this part to regulate the chemical batch reactor process's temperature. Equation (4.18) for tuning uses the same objective function for both controllers. K_p, K_i, and K_d are the three parameters of the NPID controller. The TDOF-NPID controller, on the other hand, contains five parameters: α, β, K_p, K_i, and K_d. By employing PSO, these parameters are ideally set with the goal of minimizing the performance index in Equation (4.10). The simulation employed the PSO parameters specified below.

Table 5.2 Parameters of the PSO algorithm

Parameters	NPID controllers	TDOF-NPID controller
Maximum Iteration	30	30
Swarm Size	40	40
Number of parameters	3	5
Lower Boundary	[0 0 0]	[0 0 0 0 0]
Upper boundary	[3 3 3]	[5 2 2 1 1]

Meanwhile the PID controller is tuned using the Tyreus-Luyben (TL) tuning method. The TL method is a tuning technique similar to the Ziegler-Nichols method, but with adjustments to achieve better stability in the control loop (Hassan et al., 2017). For the TL method, the relay feedback control system is constructed for the nonlinear process in Equation (3.26) and from the sustained oscillation in the test response, the ultimate gain (K_u) and the ultimate period (P_u) are obtained as K_u = 5.66 and P_u = 0.25. Then, the TL tuning formulae are (Satya, 2012).

$$K_p = K_u/3.2 \tag{5.3a}$$

$$T_i = 2.2P_u \tag{5.3b}$$

$$T_d = P_u/6.3 \tag{5.3c}$$

The table following this summarizes the PID controller tuning outcomes along with the results of the other two methods.

Table 5.3 Optimum settings of PID-TL, NPID and TDOF NPID controllers

Tuning method	Controller	Parameters				
		K_p	K_i	K_d	α	β
TL	PID	1.7684	3.2153	0.0702	-	-
IAEU	NPID	1.8512	0.4491	0.5954	-	-
	TDOF-NPID	1.0971	0.1237	0.6151	0.0046	0.0463

5.3 Results of the TDOF NPID Controller

5.3.1 Setpoint Tracking Response

To evaluate the controller's reference tracking performance, a step-type setpoint was abruptly increased from 25°C to 50°C while the system was initially at a steady state of 25°C. Figure 5.1 illustrates the resulting step responses of the TDOF-NPID controller.

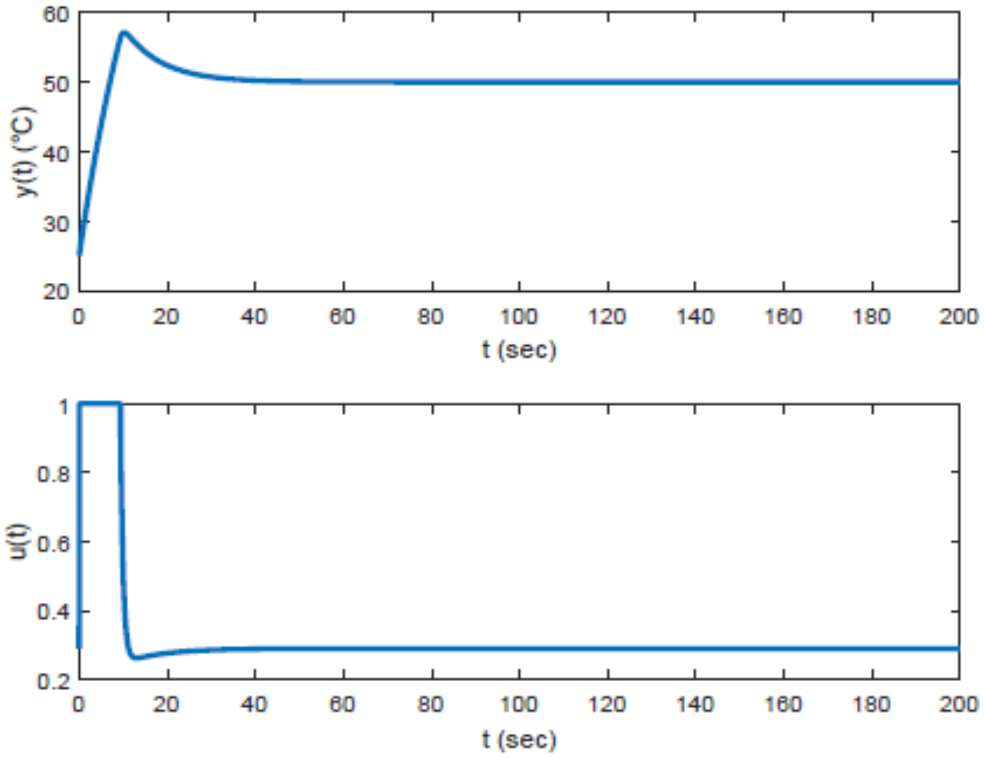

Figure 5.1Step response of the TDOF NPID controller

The output response rapidly increases from its initial state to reach the target value of 50°C. Once this desired setpoint is achieved, the output remains stable, demonstrating a high degree of accuracy and precision in maintaining the desired operating condition. This

keeping ability is crucial in ensuring the system's reliability and effectiveness in meeting its intended objectives.

The control input *u* was constrained to operate within a saturation range of 0 to 1. This limitation ensures that the control device responsible for manipulating the system's output remains within its operational boundaries. Initially, *u* rapidly increases towards its maximum value of 1 to expedite the system's response to the desired setpoint. Once the target is reached, *u* settles into a steady-state value within the saturation range, maintaining the output at the desired level while respecting the control's physical constraints. The shape of the control input might exhibit a non-linear pattern. This non-linear behavior is often necessary to effectively control systems with non-linear characteristics. Despite the non-linear control action, the controller is successfully tracking the setpoint and maintaining a stable output. This indicates that the TDOF NPID controller is well-suited for the specific system dynamics, even when dealing with non-linear elements. The result demonstrates the successful setpoint tracking of the controller. The controller effectively regulates the output response while adhering to control input constraints.

5.3.2 Disturbance Rejection Response

Another simulation was conducted to assess the system's disturbance rejection capabilities. Since all variables, input, and output signals in this simulation are dimensionless, a dimensionless disturbance was introduced to reactor temperature to simulate variations in control system instability. The disturbance was randomly generated between 0 and 1, with 0 representing no disturbance and 1 representing the maximum disturbance. A unity disturbance was introduced to the system's input at the start of the simulation, while maintaining the initial output at 50°C. Figure 5.2 depicts the TDOF NPID controller's disturbance rejection performance.

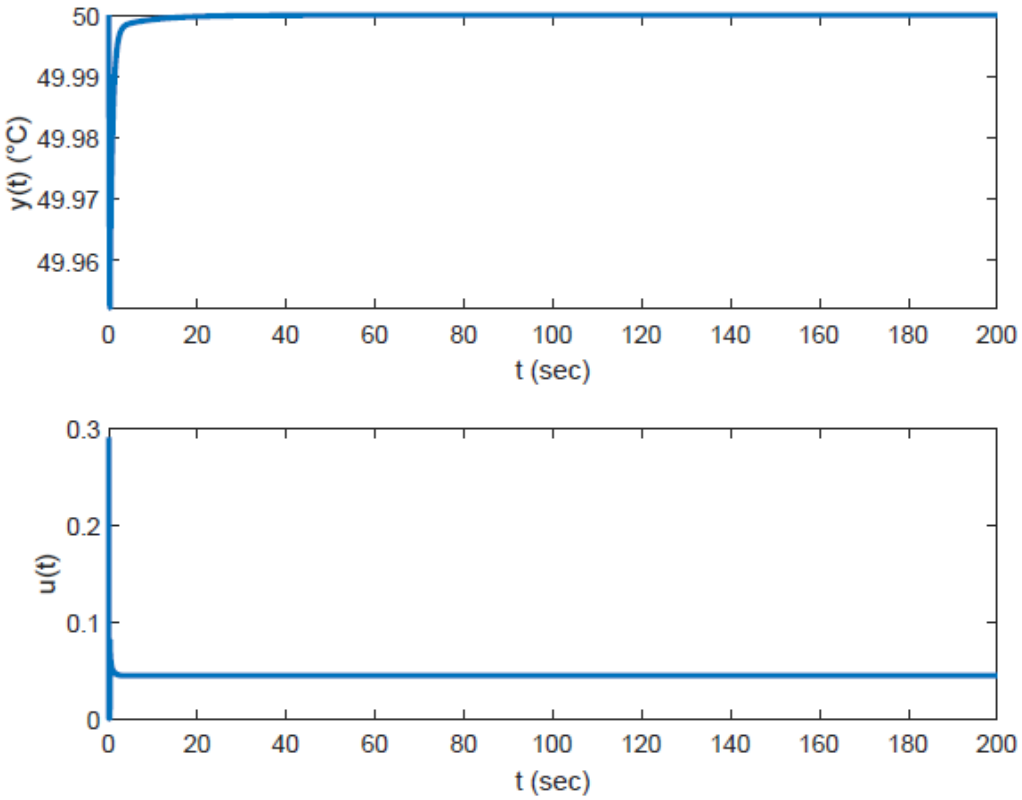

Figure 5.2 Disturbance rejection response of the TDOF NPID

The primary objective is to evaluate the system's ability to effectively reject the disturbance and maintain the output at the desired target value of 50°C. This simulation provided valuable insights into the controller's performance under challenging conditions. The controller reacts quickly to the disturbance, with the control input *u* exhibiting a sharp increase. This indicates the controller's immediate action to counteract the disturbance. The output response *y* experiences a temporary deviation but subsequently returns to its original steady-state value, demonstrating the controller's effectiveness in rejecting the disturbance. The shape of the control input suggests that the TDOF-NPID controller is actively adjusting its output to handle the disturbance. This nonlinear behavior is likely essential for effectively compensating for the system's nonlinearities.

The controller demonstrates robust disturbance rejection capabilities. It responds promptly to the disturbance, effectively returning the output to its desired setpoint. The nonlinear control action likely plays a crucial role in achieving this performance, especially in systems with complex dynamics.

5.4 Results of the NPID Controller

5.4.1 Setpoint Tracking Response

The following figure illustrates the setpoint tracking performance of the NPID controller. The top graph shows the output response, while the bottom graph depicts the control input over time. Initially, the output is 25°C lower than the target temperature.

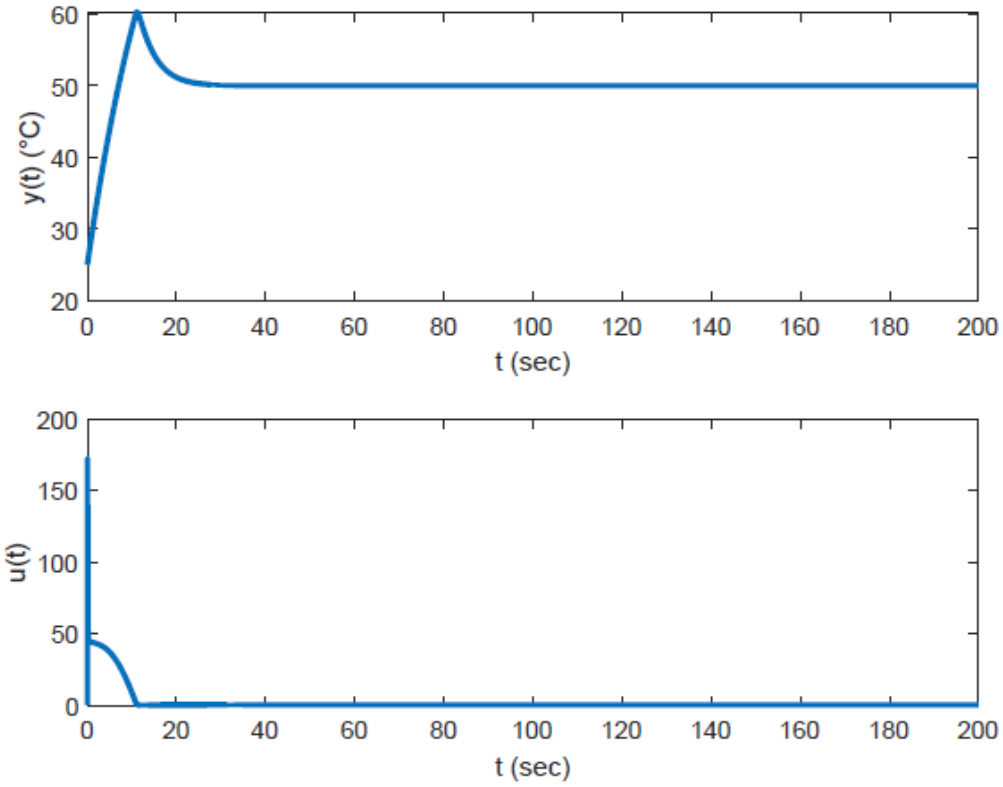

Figure 5.3 Step responses of the NPID controller

The output response starts at a value below the desired setpoint. This indicates that the system is initially in a steady state that is different from the desired operating condition. A setpoint change is likely introduced at time $t = 0$, as evidenced by the rapid increase in the output response. The controller immediately takes action to drive the output towards the new setpoint. The control input u initially exhibits a sharp rise, indicating an aggressive effort to bring the output to the desired value. This rapid increase is likely due to the proportional and derivative terms in the NPID controller. As the output approaches the setpoint, the integral term in the NPID controller becomes more active, providing a steady-state error correction. The observed behavior of the NPID controller suggests that it employs a nonlinear gain strategy that saturates the control input and adapts the gain to reduce it as the error decreases.

This adaptive nonlinear gain allows for a smoother and more refined control action, contributing to the overall performance of the controller. The controller demonstrates effective setpoint tracking, with a relatively quick response to the setpoint change and minimal steady-state error. The nonlinear control action likely plays a crucial role in achieving this performance, especially in systems with complex dynamics.

5.4.2 Disturbance Rejection Response

For disturbance rejection test, a unity disturbance was introduced to the system's input at the start of the simulation while the system was maintaining at the desired setpoint of 50°C. Figure 5.4 depicts the disturbance rejection response of the NPID controller.

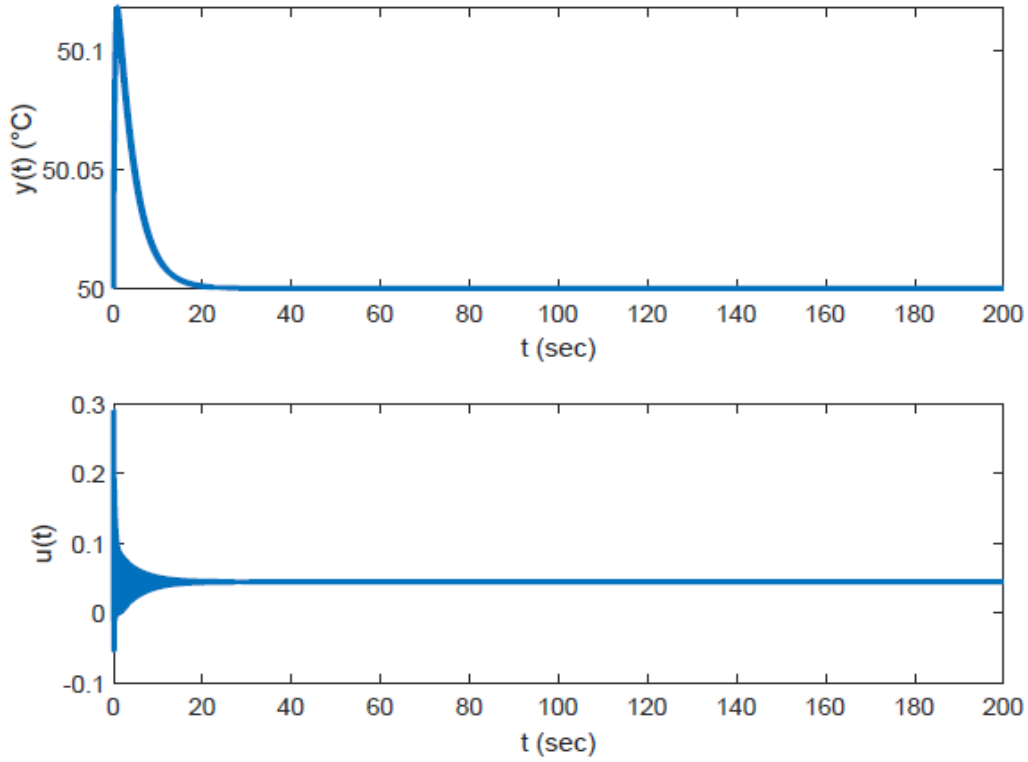

Figure 5.4 Disturbance rejection of the NPID controller

As evidenced by the sudden deviation in the output response, the controller reacts promptly to the disturbance, with the control input exhibiting a sharp increase. This indicates the controller's immediate action to counteract the effects of the disturbance. The output response experiences a temporary deviation but subsequently returns to its original steady-state value, demonstrating the controller's effectiveness in rejecting the disturbance. The shape of the control input suggests that the NPID controller is actively adjusting its output

to handle the disturbance. This nonlinear behavior is likely essential for effectively compensating for the system's nonlinearities.

The controller effectively handles disturbances, swiftly returning the output to its desired value. This performance is likely attributed to the nonlinear control strategy, particularly in systems with intricate dynamics.

5.5 Results of the PID Controller

5.5.1 Setpoint Tracking Response

Figure 5.5 shows the setpoint tracking response of the PID controller tuned using the Tyreus-Luyben method. The output response starts at a value of 25°C below the desired setpoint.

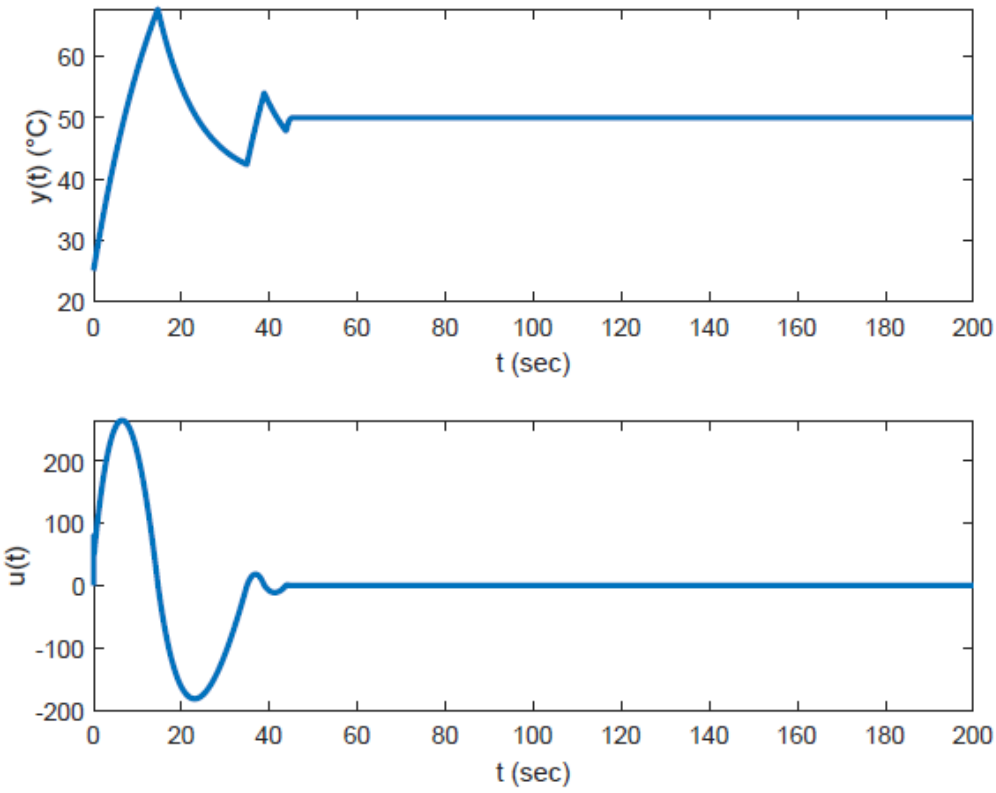

Figure 5.5Step responses of the PID controller

This suggests that the system is currently stable but operating at a point that deviates from the desired target. The controller swiftly responds to a sudden change in the desired output, initiating a rapid increase in the control signal. This initial surge is likely attributed to the proportional and derivative components of the controller. As the output nears the desired value, the integral component becomes more influential, gradually reducing the control

signal. However, a slight steady-state error may persist, indicating a minor discrepancy between the actual and desired output. The controller effectively maintains the desired output level, responding promptly to changes and exhibiting acceptable steady-state errors. To fully understand its performance and identify potential enhancements, a more in-depth examination of its tuning settings and the system's characteristics is warranted.

5.5.2 Disturbance Rejection Response

The disturbance rejection capabilities of the PID controller, tuned with the Tyreus-Luyben method (TL), are shown in Figure 5.6.

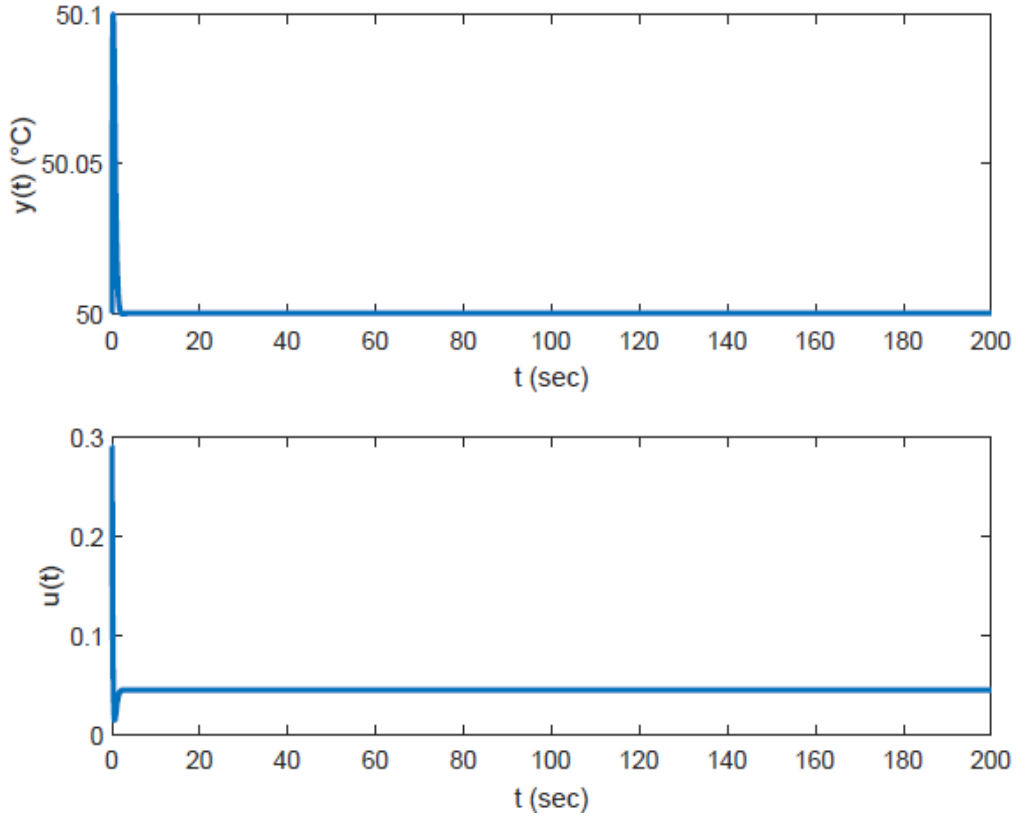

Figure 5.6 Disturbance Rejection of PID-TL controller

While the system was in a steady-state of 50°C at the beginning of the simulation, a unity disturbance was introduced at $t = 0$. The controller reacts promptly to the disturbance, with the control input exhibiting a sharp increase. This indicates the controller's immediate action to counteract the effects of the disturbance. The output response experiences a temporary deviation but subsequently returns to its original steady-state value, demonstrating the controller's effectiveness in rejecting the disturbance. The controller demonstrates robust disturbance rejection capabilities.

5.6 Performance Comparison of the Three Controllers

5.6.1 Setpoint Tracking Performance

As discussed before, to conduct a setpoint tracking test, the step-type setpoint was changed to 50°C when the process was kept at 25°C. Figure 5.7 illustrates the step responses of the three controllers where *y(t)* represents the temperature measured in degrees Celsius at time *t*, where *t* is expressed in seconds.

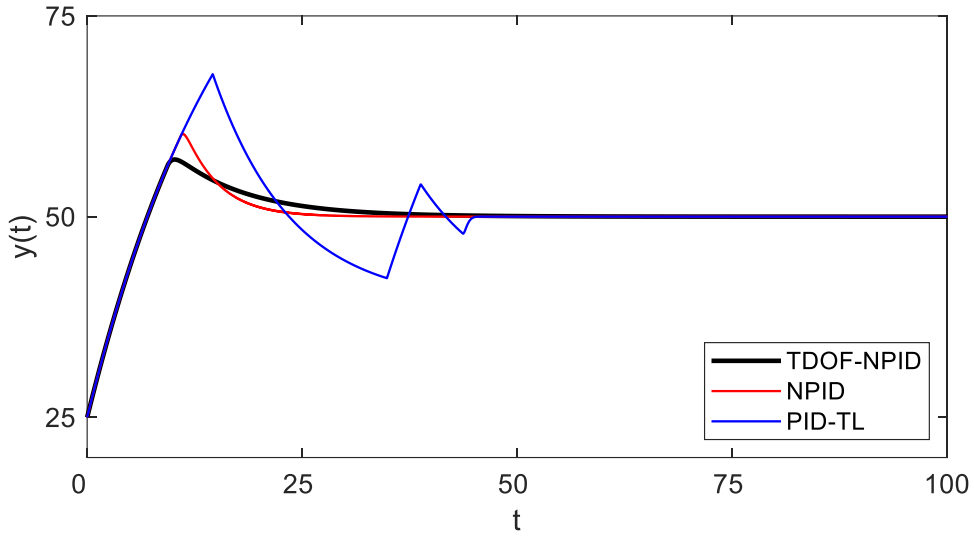

Figure 5.7 The three controllers' step responses

Equation (5.1) was used to compute the overshoot (M_p), settling time (t_s), and IAE in order to compare the three controllers' abilities quantitatively. Table 5.3 compares the results and the TDOF NPID controller achieved an overshoot of 28.46 %, a settling time of 25.51 seconds, and an IAE of 159.37, while the NPID and PID controllers achieved overshoots of 41.27 % and 70.96 %, settling times of 19.85 seconds and 44.10 seconds, and IAEs of 148.78 and 293.73, respectively.

In a chemical reactor, maintaining the reactor temperature around operating temperature is essential for ensuring optimal reaction rate, product quality, energy efficiency, safety, and overall process control. Since a slight temperature change can significantly alter the reaction speed, even if the reaction is a bit slow, the overshoot should be as small as possible. The TDOF NPID demonstrated the lowest M_p value of 28.46% with resonable t_s and IAE compared to the NPID controller. This indicates that the TDOF NPID controller is the most suitable controller.

Table 5.4 Setpoint tracking performance of the three controllers

Controller	Performance		
	M_p	t_s	*IAE*
TDOF-NPID	28.46	25.51	159.37
NPID	41.27	19.85	148.78
PID	70.96	44.10	293.73

5.6.2 Disturbance Rejection Performance

A dimensionless disturbance was applied to the reactor temperature to model variations in control system stability. This disturbance, randomly chosen between 0 and 1, represented a range from no disturbance to maximum disturbance. As done previously, a simulation was conducted to add dimensionless disturbance *d* by 1 to the input term to check the system's disturbance rejection performance while the output stays at 50°C at *t*= 0sec. The disturbance rejection responses of the three approaches are can be seen in the subsequent figure.

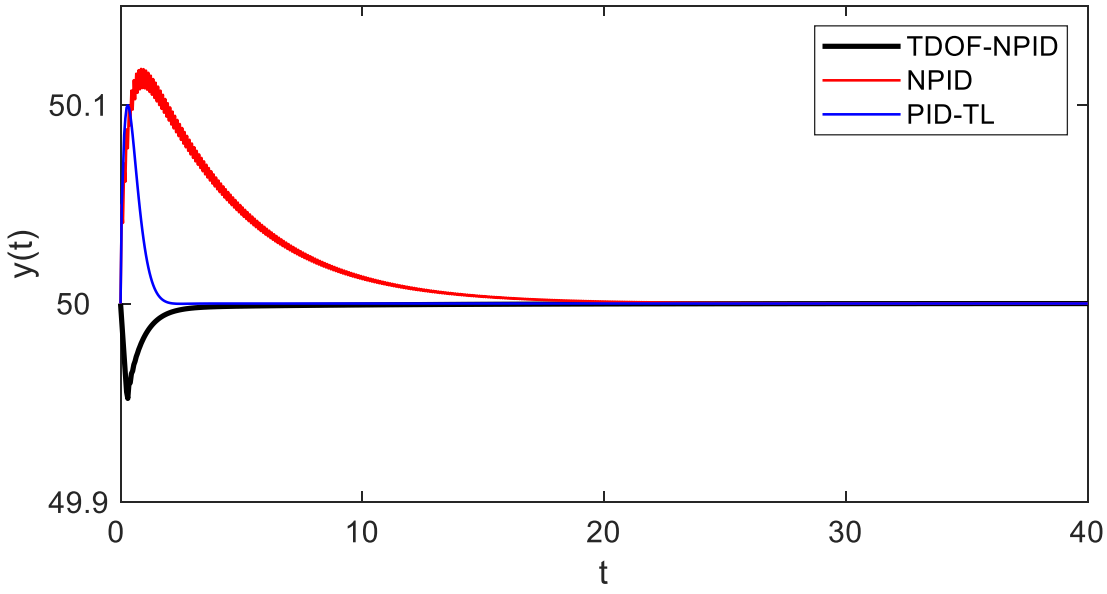

Figure 5.8 Disturbance rejection responses of the three controllers

The integral of absolute error (IAE), recovery time (t_{rcy}), and perturbance peak (M_{peak}) are used to quantify the performance of disturbance rejection. Within 2% of y_s, M_{peak} indicates $|y_{max}-y_s|$ or $|y_{min}-y_s|$, and T_{rcy} measures the amount of time it takes for y to recover.

Based on the provided result, the TDOF-NPID controller exhibits superior performance with the lowest M_{peak}, indicating better overshoot suppression, smaller IAE, and reasonable t_{rcy} compared to both the NPID and PID-TL controllers. This indicates its ability to effectively maintain a constant operating temperature, even in the face of external disturbances. The PID controller demonstrated a reasonable balance between performance metrics, while the NPID controller showed the poorest performance in terms of overshoot and settling time.

Table 5.5 Disturbance rejection performance of the three controllers

Controller	**Performance**		
	M_{peak}	t_{rcy}	*IAE*
TDOF-NPID	0.05	2.89	0.05
NPID	0.12	13.25	0.59
PID	0.10	1.52	0.08

CHAPTER SIX

CONCLUSION AND RECOMMENDATION

6.1 CONCLUSION

This research involved a comprehensive review of existing literature on batch processes and the subsequent development of a mathematical model for both the plant and the proposed controller. Due to the model's complexity, dimensionless equations were derived to simplify the analysis. While batch processes operate dynamically, understanding potential steady states can inform the development of control strategies. However, the dynamic nature of batch reactors necessitates a focus on transient behavior for accurate modeling and control. Batch processes undergo deliberate changes in state variables over time, aiming for a desired final state or target condition rather than a constant equilibrium.

This study introduces TDOF NPID controller. The primary objective of this study is to evaluate the effectiveness of a TDOF NPID controller in regulating the temperature of a batch reactor. The controller's performance will be assessed based on its ability to achieve accurate setpoint tracking, minimize overshoot and settling time, and demonstrate robust disturbance rejection. PSO was used to optimize the controller's parameters with the goal of minimizing the IAEU. The lowest IAE value attained was used to determine the gains for the controller. The proposed system was compared to two established controllers, Nonlinear PID and PID-TL. The comparison focused on setpoint tracking and disturbance rejection performance, evaluating parameters such as settling time, overshoot, rise time, and IAE.

The suggested controller was chosen above the other controllers under consideration because its setpoint control performance showed the least amount of overshoot (28.46%) while maintaining a reasonable settling time and integral absolute error (IAE). When subjected to a dimensionless disturbance of d=1 at the input, the proposed controller demonstrated exceptional disturbance rejection capabilities. It exhibited the lowest overshoot of 0.05% while maintaining an acceptable settling time of 2.89 seconds and an integral absolute error of 0.05. This performance shows how well the controller can keep the operating temperature steady even when there are outside disruptions.

In comparison, the PID controller offered a balanced performance, while the NPID controller exhibited the highest overshoot and slowest settling time.

This research developed a TDOF-NPID controller, conducted a comparative analysis with existing controllers, and evaluated the responses using IAEU minimization. Overall, the outcomes show how much the suggested controller performs.

6.2 RECOMMENDATION

This research introduces a TDOF-NPID controller for regulating the temperature of a batch reactor. While simulated data was used for this study, real-world testing is recommended for further validation. To simplify the model, concentration control was omitted, but a cascade control structure incorporating both temperature and concentration is suggested for future work.

REFERENCES

Ahmed, E. (2013). Hydrogel: Preparation, characterization, and applications: A review. *Journal of Advanced Research*, *6*. https://doi.org/10.1016/j.jare.2013.07.006

Almabrok, A., Dounis, A., & Psarakis, M. (2018). Fast tuning of the PID controller in an HVAC system using the Big Bang-Big Crunch algorithm and FPGA technology. *Journal of Algorithms*, *11*, 146. https://doi.org/10.3390/a11100146

Araki, M. (1984). PID control system with reference feedforward (PID-FF control system). *Proc. 23rd SICE (Society of Instrument and Control Engineers) Annual Conference*, 31–32.

Araki, M., & Taguchi, H. (2003). Two-degree-of-freedom PID controllers. *International Journal of Control, Automation, and Systems*, 401–411.

Balaton, M. G., Nagy, L., & Szeifert, F. (2013). Jacket temperature control of a batch reactor using three different temperature levels. *Industrial & Engineering Chemistry Research*, 1939–1946.

Borase, R. P., Maghade, D. K., Sondkar, S. Y., & Pawar, S. N. (2021). A review of PID control, tuning methods and applications. *International Journal of Dynamics and Control*, *9*, 818–827.

Chen, C. T. (2014). A sliding mode control strategy for robust temperature trajectory tracking of a batch reactor. *Chemical Engineering Communications*, 1–22.

Chen, C. T., & Peng, S. T. (1998). A simple adaptive control strategy for temperature trajectory tracking in batch processes. *The Canadian Journal of Chemical Engineering*, 1118–1127.

Conesa, J. A. . (2020). *Chemical reactor design : mathematical modeling and applications*. Wiley-VCH.

Doble, M. (2007). Perry's chemical engineers' handbook. *McGraw-Hil, New York, US*.

Gharagozloo, M. H., Ghasemi, R., & Sedighi, M. (2020). Nonlinear Model Predictive Versus Sliding Mode Controller Design for a Class of Nonlinear Non-Affine Chemical Batch Reactor Dynamics. *EasyChair Preprint: Budapest, Hungary*.

Ghasem, N. M., Hussain, M. A., & Sata, S. A. (2006). Application of model predictive control to batch polymerization reactor. *Revista de La Facultad de Ciencias*, *11*(1), 49–58.

Gilbert F. Froment, Kenneth B. Bischoff, & Juray De Wilde. (2011). *Chemical Reactor Analysis and Design*.

Global, F. (2023). *DS 7-46 Chemical Reactors and Reactions (Data Sheet)*.

Haan, A. B. (2015). Chemical reactors and their industrial applications. *Process Technology; De Gruyter: Berlin, Germany; Munich, Germany; Boston, MA, USA*, 51–78.

Halim, A. H., & Ismail, I. (2019). Tree physiology optimization on SISO and MIMO PID control tuning. *Neural Computing and Applications*, *31*(11), 7571–7581.

Hassan, A. A., Al-Shamaa, N. K., & Abdalla, K. K. (2017). Comparative study for DC motor speed control using PID controller. *International Journal of Engineering and Technology*, *9*(6), 4181–4192.

Hill, C. G., & Root, T. W. (2014). *Introduction to chemical engineering kinetics and reactor design*. John Wiley & Sons.

Jin, G.-G., & Son, Y.-D. (2019). Design of a nonlinear PID controller and tuning rules for first-order plus time delay models. *Studies in Informatics and Control*, *28*(2), 157–166.

Jutan, A., & Uppal, A. (1984). Combined feedforward-feedback servo control scheme for an exothermic batch reactor. *Industrial & Engineering Chemistry Process Design and Development*, *23*(3), 597–602.

Kadu, C. B., Khandekar, A. A., & Patil, C. Y. (2018). Design of sliding mode controller with proportional integral sliding surface for robust regulation and tracking of process

control systems. *Journal of Dynamic Systems, Measurement, and Control*, *140*(9), 091004.

Kanavalau, A., Masters, R., Kähm, W., & Vassiliadis, V. S. (2019). Robust thermal stability for batch process intensification with model predictive control. *Computers & Chemical Engineering*, *130*, 106574. https://doi.org/10.1016/j.compchemeng.2019.106574

Korotkin, S., Zaidner, G., Shteimberg, E., Ellenbogen, A., Arad, M., & Cohen, Y. (2010). Non Linear PID and its application in Process Control. *IEEE 26-Th Convention of Electrical and Electronics Engineers in Israel* , 574–577.

Levenspiel, O. (2013). *Chemical Reactor Omnibook-soft cover*. Lulu. com.

Mann, U. (2009). Principles of chemical reactor analysis and design. *New Tools for Industrial Chemical Reactor Operations. John Wiley & Sons.*

Mishra, C. K., Jebakumar, J. S., & Mishra, B. K. (2014). Controller selection and sensitivity check on the basis of performance index calculation. *International Journal of Electrical, Electronics and Data Communication*, *2*(1), 91–93.

Missen, R. W., Mims, C. A., & Saville, B. A. (1999). *CHEMICAL REACTION*.

Moran, S., & Henkel, K. (2000). Reactor types and their industrial applications. *Ullmann's Encyclopedia of Industrial Chemistry*, 1–49.

Narwekar, K., & Shah, V. A. (2020). Temperature control using sliding mode control: an experimental approach. *Information and Communication Technology for Sustainable Development: Proceedings of ICT4SD 2018*, 531–538.

Niu, L., & Yang, D. (2013). Dynamic simulation and optimization for batch reactor control profiles. *Fifth International Conference on Machine Vision (ICMV 2012): Algorithms, Pattern Recognition, and Basic Technologies*, *8784*, 486–489.

O'dwyer A. (2009). Handbook of PI and PID controller tuning rules. *World Scientific.*

Oliveira, E. J., Honorio, L. M., Anzai, A. H., & Soares, T. X. (2014). Linear programming for optimum PID controller tuning. *Applied Mathematics*, *2014*.

Podofillini, L., & Dang, V. N. (2012). Conventional and dynamic safety analysis: Comparison on a chemical batch reactor. *Reliability Engineering & System Safety*, *106*, 146–159.

Ravi, R. (2017). Reactor Design—General Principles. In *Coulson and Richardson's Chemical Engineering* (pp. 1–101). Elsevier.

Ray, W. H., & Szekely, J. (1973). Process optimization. *With Applications in Metallurgy and Chemical Engineering*.

Schmidt, L. D. (2005). *The engineering of chemical reactions*. Oxford University Press New York.

Scott Fogler, H. (2016). *The grid: elements of chemical reaction engineering*. Prentice Hall.

Shamsuzzoha, M., & Raja, G. L. (2023). *PID Control for Linear and Nonlinear Industrial Processes*.

Shuaib, A., & Ahmed, M. (2014). Robust PID control system design using ITAE performance index (DC motor model). *International Journal of Innovative Research in Science, Engineering and Technology*, *03*, 15060–15067. https://doi.org/10.15680/IJIRSET.2014.0308002

Shuler, M. L. (1992). Bioprocess enzineering. *Prentice-Hall*, 412–420.

Skogestad, S. (2008). *Chemical and energy process engineering*. CRC press.

Smith, R. (2005). *Chemical process: design and integration*. John Wiley & Sons.

Štampar, S., Sokolič, S., & Karer, G. (2013). Nonlinear control of a hybrid batch reactor. *Strojniški Vestnik-Journal of Mechanical Engineering*, *59*(2), 112–123.

Su, Y. X., Sun, D., & Duan, B. Y. (2005). Design of an enhanced nonlinear PID controller. *Mechatronics*, *15*(8), 1005–1024.

Toledo, & Mettler. (2024). *Jacketed Reactors*. https://www.mt.com/nz/en/home/products/L1_AutochemProducts/automated-reactor-control-systems/jacketed-reactors.html

Tominaga, H., & Tamaki, M. (1997). Chemical reaction and reactor design. *(No Title)*.

University of Michigan College of Engineering. (2022). *Batch*. https://encyclopedia.che.engin.umich.edu/batch/

Xiao, J., Shao, C., Zhu, L., & Song, T. (2015). Batch reactor temperature control based on DMC-optimization PID. *IEEE International Conference on Cyber Technology in Automation, Control, and Intelligent Systems (CYBER)*, 371–376.

Yadav, E. S., Shettigar J, P., Poojary, S., Chokkadi, S., Jeppu, G., & Indiran, T. (2021). Data-Driven Modeling of a Pilot Plant Batch Reactor and Validation of a Nonlinear Model Predictive Controller for Dynamic Temperature Profile Tracking. *ACS Omega*, *6*(26), 16714–16721. https://doi.org/10.1021/acsomega.1c00087

Zhang, H., & Hu, B. (2012). The application of nonlinear PID controller in generator excitation system. *Energy Procedia*, *17*, 202–207.

Zhang, Z., Wu, Z., Durand, H., Albalawi, F., & Christofides, P. D. (2018). On integration of feedback control and safety systems: Analyzing two chemical process applications. *Chemical Engineering Research and Design*, *132*, 616–626.

Appendix

A: For Model of Batch Reactor Dynamics

Code for relationship between concentrations

```
%% function plot_ABC_concentrations

% Parameters
k1 = 0.1; % Rate constant for A → B
k2 = 0.2; % Rate constant for B → C
Ca0 = 1; % Initial concentration of A
Cb0 = 0; % Initial concentration of B
Cc0 = 0; % Initial concentration of C
tspan = [0 10]; % Time span

% Initial conditions
y0 = [Ca0; Cb0; Cc0];

% ODE function
function dydt = reaction_model(t, y)
    Ca = y(1);
    Cb = y(2);
    Cc = y(3);
    dCadt = -k1 * Ca;
    dCbdt = k1 * Ca - k2 * Cb;
    dCcdt = k2 * Cb;
    dydt = [dCadt; dCbdt; dCcdt];
end

% Solve the ODE
[t, y] = ode45(@reaction_model, tspan, y0);

% Extract concentrations
```

```
Ca = y(:, 1);
Cb = y(:, 2);
Cc = y(:, 3);

% Plot the results
plot(t, Ca, 'b', t, Cb, 'r', t, Cc, 'g');
xlabel('Time');
ylabel('Concentration');
legend('A', 'B', 'C');
end
```

Code for Model of Batch Process

```
function xdot= BatchReactor(t,x,u,d)
% BatchReactor: Simulates a batch reactor process
% Inputs:
%   t: Time
%   x: State vector [Ca; Cb; Cc]
%   u: Control input
%   d: Disturbance
% Outputs:
%   xdot: Time derivative of the state vector

A10= 1.1; A20= 172.2; E1= 20900; E2= 41800;
R= 8.3143; Tc= 25;
r1= 41.8; r2= 83.6;
a1= 4.3145; a2= -0.1099;
b1= 1.4962; b2= 0.0515;

xdot= zeros(3,1);
k1= A10*exp(-E1/(R*x(3)));
k2= A20*exp(-E2/(R*x(3)));
xdot(1)= -k1*x(1)^2;
```

```
xdot(2)= k1*x(1)^2-k2*x(2);
xdot(3)= r1*k1*x(1)^2+r2*k2*x(2)+a1+a2*x(3)+(b1+b2*x(3))*u+d;
end
```

B. Evaluation performance of TDOF NPID Controller

Code for setpoint tracking

```
% Measure IAEU performance of the TDOF_NPID control system
% x= [Kp Ki Kd a b]: Controller parameters
% graph: 1 for drawing the graph
function IAEU= EvalObj_TDOF_NPID_SP(x,graph)

% Clear the persistent variables in the TDOF_NPID controller
clear TDOF_NPID

% Controller parameters
N= 10;
gains= [x N];

% Reactor parameters
a1= 4.3145; a2= -0.1099;
b1= 1.4962; b2= 0.0515;

% Other parameters
t= 0; h= 0.05; x= [0;0;25]; y= x(3); yr= 50; d= 0.0; % Disturbance
loop= 4000; dyr= d;

u0= -(a1+a2*yr)/(b1+b2*yr); % Control input in the steady-state

buf= [t x' u0 u0];

for i= 1:loop

   % Calls the TDOF_NPID controller
```

```
    u= TDOF_NPID(yr,y,h,gains,dyr,0);

    % Limits the control input
    usat= min(max(u,0),1);

    % Calls the process model
    x= RK4(@BatchReactor,t,x,usat,h,d);
    y= x(3);
    t= t+h;
     % Check for simulation termination
    if t >=200
        break;
    end

    buf= [buf;t x' u usat];
    if abs(y) > 1e+7
        break;
    end
end

% Calculates the performance
e= yr-buf(:,4); du= buf(:,5)-u0; w= 0; % Weighting factor
ae= abs(e)+w*abs(du); % IAEU
IAEU= 0.5*h*(ae(1)+2*sum(ae(2:end-1))+ae(end));

% Plots the response
```

Code for disturbance rejection response

```
function IAEU= EvalObj_TDOF_NPID_DIS(x,graph)

% Clear the persistent variables in the TDOF_NPID controller
clear TDOF_NPID
```

```
% Controller parameters
N= 10;
gains= [x N];

% Calls Reactor parameters

% Other parameters
t= 0; h= 0.05; x= [0;0;50]; y= x(3); yr= 50; d= 1; % Disturbance
loop= 4000;  dyr= 2*d;

u0= -(a1+a2*yr)/(b1+b2*yr); % Control input in the steady-state

buf= [t x' u0 u0];

for i= 1:loop

   % Calls the TDOF_NPID controller
   u= TDOF_NPID(yr,y,h,gains,dyr,u0);

   % Limits the control input
   usat= min(max(u,0),1);

   % Calls the process model
   x= RK4(@BatchReactor,t,x,usat,h,d);
   y= x(3);
   t= t+h;
    % Check for simulation termination
   if t >= 200
      break;
   end

   buf= [buf;t x' u usat];
   if abs(y) > 1e+7
```

```
        break;
    end
end

% Calculates the IAEU performance
e= yr-buf(:,4); du= buf(:,5)-u0; w= 0; % weighting factor
ae= abs(e)+w*abs(du);
IAEU= 0.5*h*(ae(1)+2*sum(ae(2:end-1))+ae(end));

% Plots the response
```